Photochemistry on Metal Nanoparticles

Kazuo Watanabe,*,† Dietrich Menzel,†,‡ Niklas Nilius,† and Hans-Joachim Freund†

Fritz-Haber-Institut der Max-Planck-Gesellschaft Faradayweg 4-6, 14195 Berlin, Germany and Fakultät für Physik E20, Technische Universität München, 85747 Garching, Germany

Received January 23, 2006

Contents

1. Introduction

The photochemistry of small molecules on well-defined metal surfaces has been the subject of intense research for more than three decades.[1] This field is of interest because it rests on the superposition of two influences. On one hand, new reaction channels can become possible by electronic excitation, which are usually not accessible by thermal activation. On the other hand, compared to molecular photochemistry in the gas phase, interactions of molecules with solid substrates open unique pathways of photoexcitation and photoreaction not accessible in homogeneous reactions. This is primarily due to the fact that the bonding interactions with the substrate modify not only the ground state but also the electronically excited states of the adsorbates. In addition, the very rapid exchange of excitation energy between adsorbates and substrate, in particular on metal and semiconductor surfaces, can lead to fast quenching of excited adsorbate states by transfer of charge and/or energy from the adsorbates to the substrate. Furthermore, excitation of adsorbates by hot (excited) electrons produced by photoabsorption in the substrate plays an important role as it induces charge and energy transfer in the opposite direction, from the substrate to adsorbates. Well-defined metal surfaces covered by adsorbate layers under ultrahigh vacuum (UHV) conditions provide systems which are well characterized in all aspects, particularly regarding geometry and electronic structure. The fact that such layers usually consist of molecules which are naturally aligned on the surface[2] makes surface photochemistry a powerful alternative to the stereodynamic control of chemical reactions by optically aligned molecular beams.[3] Well-defined adsorbate systems thus provide unique playgrounds for surface photochemistry.

Stimulated by the demand to bridge the gap between surface science under UHV conditions and processes on real catalysts, model systems for heterogeneous catalysis have been extensively studied in the past decade. Such systems usually consist of nanometer-sized metal particles supported on thin oxide layers.[4−9] The purpose of these studies is not only detailed exploration of real catalysts but also the desire to better control the physical, chemical, and catalytic properties of nanoparticle systems. Here we use the term metal nanoparticle (MNP) for metallic particles with sizes in the nanometer range. The term metal cluster is also frequently used, more or less in an interchangeable manner. However, this term is generally used for a broader size range, starting from very small aggregates containing 3 atoms (trimer) up to particles of micrometer diameter.[10] For physical aspects of metal clusters on solid surfaces, readers are referred to refs 11−13. The small clusters which show effects of molecular and shell structures will not be important in our context. Synthesis and applications of size-controlled ligand-stabilized MNPs, such as Au_{55}, constitute a large research field;[14−16] however, they are also outside the scope of the present review.

Thermally driven chemical reactions have been studied on mass-selected metal clusters in the gas phase[17] and after soft landing onto solid surfaces.[18] In the latter case even catalytic cycles have been observed. [19−22] In contrast, there are very few studies on the photochemistry of molecules adsorbed on metal clusters in the gas phase.[23,24] To our knowledge, the photocatalytic properties of mass-selected metal clusters soft-landed on surfaces have not been investigated so far. The latter approach of depositing small, mass-selected clusters onto substrates and investigating their size-specific properties can be referred to as a 'bottom-up method', which would allow the highest degree of control if one could determine the surface quality and densities of

* To whom correspondence should be addressed. E-mail: watanabe@fhi-berlin.mpg.de.
† Fritz-Haber-Institut der Max-Planck.
‡ Technische Universität München.

10.1021/cr050167g CCC: $59.00
Published on Web 09/12/2006

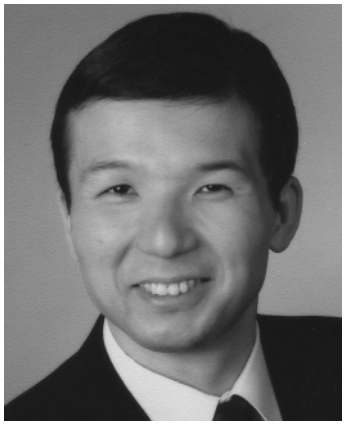

Kazuo Watanabe was born in 1969 in Tokyo. He received his B.Eng. degree in Chemistry from the University of Tokyo in 1993. He did his Ph.D. studies on the photochemistry of methane on transition-metal surfaces with Yoshi Matsumoto at the Institute for Molecular Science (IMS). He received his Ph.D. degree in Chemistry from the Graduate School of Advanced Studies in 1998 and then worked as a research associate at IMS and the University Tokyo, where he studied the photochemistry and photophysics of molecular clusters in the gas and liquid phases and metal nanoparticles deposited on surfaces by using various methods including ultrafast time-resolved absorption spectroscopy, state-resolved photofragment imaging, and scanning tunneling microscopy/spectroscopy. Since 2004 he has been a workgroup leader in Hajo Freund's group at the Fritz-Haber-Institute. His current research interests focus on photon- and plasmon-induced chemical and physical processes on metal nanostructures.

Dietrich Menzel was born in 1935 in Marienbad (then Czechoslovakia). He studied chemistry at the Technische Hochschule Darmstadt and received his Ph.D. degree in 1962 for basic catalytic studies. He was a postdoctoral fellow with Robert Gomer at the University of Chicago from 1962 to 1964 using field emission microscopy to study electronically induced desorption, which led to the proposal of a basic mechanism. From 1964 to 1969 he built a small group at Technische Hochschule Darmstadt working on energy transfer and electronically induced processes at surfaces. In 1969 he went to the Physical Chemistry Institute of the Technische Hochschule (later Technische Universitaet) Muenchen, where he continued his surface science work. In 1973 he accepted a chair in physics at this university where he led a group working on the geometrical, vibrational, and electronic structure of adsorbate and coadsorbate systems on single-crystal surfaces as well as their dynamics and kinetics. Since his retirement in 2003 he has continued to work in these fields in collaboration with various groups. In 2004 he became a consultant for a group in the Fritz-Haber Institut in Berlin (where he has been an external scientific member since 1989), working on the photochemistry of metallic nanoparticles.

Niklas Nilius was born in 1971 in Halle/Saale, Germany. He studied physics at the universities of Jena and Halle and received his diploma in the group of H. Neddermeyer in 1997. For his Ph.D. work he joined the group of H.-J. Freund in Berlin, where he studied the optical properties of single metal particles by analyzing the light emission from the tunneling contact of an STM. Between 2002 and 2003 he worked as a postdoctoral fellow with Wilson Ho on the properties of atomic chains artificially assembled by STM. He returned to H.-J. Freund's group as a group leader and is now in charge of the STM experiments.

Hans-Joachim Freund (born 1951) studied physics and chemistry at the University of Cologne and received his Ph.D. degree in 1978 with a thesis on quantum chemical calculations and spectroscopic studies on transition-metal carbonyl compounds in comparison with carbon monoxide adsorbates. Between 1979 and 1981 he worked in the Physics Department at the University of Pennsylvania as a postdoctoral fellow on synchrotron studies of the electronic structure of adsorbates. After having returned to Cologne he finished his habilitation in 1983 and accepted in the same year a position as associate professor at the University Erlangen-Nürnberg. In 1987 he moved to a position as full professor for physical chemistry at the Ruhr-Universität Bochum. In 1995 he accepted a position as a scientific member and director at the Fritz-Haber-Institut der Max-Planck-Gesellschaft in Berlin, where he is Head of the Department of Chemical Physics. He serves as Adjunct Professor of the Ruhr-Universität in Bochum and of the Freie Universität, Technische Universität, and Humboldt Universität in Berlin. In 1995 he received the Gottfried Wilhelm Leibniz Award of the German Science Foundation (DFG) and is a recipient of the Centenary Medal and Lecture of the Royal Society of Chemistry. He is an ordinary member of the Chemical Sciences Section of the Academia Europea, the Berlin-Brandenburgische Akademie der Wissenschaften, as well as a Foreign Member of Brazilian Academy of Science. He has been a fellow of the American Physical Society since 2001. He is a member of several scientific societies and several advisory boards of scientific journals and has published more than 480 scientific papers.

specific defects with a very high degree of precision. Since this is generally not the case one has to characterize the system after cluster deposition, and this is typically not practiced, in particular not for oxide surfaces. Characterization by STM was, however, attempted for small metal clusters of up to several tens of atoms on Pt(111),[25−27] Si(111),[28−30] and graphite[31] surfaces. An alternative approach is the vapor deposition of metal atoms on substrates, followed by aggregation into crystalline or amorphous NPs. This

technique shows the highest flexibility in forming particle systems with various topographic and electronic properties and allows the study of size-selected, deposited clusters by local probe spectroscopies. In both approaches the comparison between experimental and theoretical results as well as with data obtained on planar surfaces is of highest interest and importance, in particular when the presence of NPs leads to qualitatively new phenomena, such as particle size effects, cluster−support interactions, or specific collective excitations in the single MNP or in the ensemble.

In Table 1 we compare the characteristic properties of single-crystal metal surfaces and supported metal NPs. The latter shows a variety of new physical and chemical properties in addition to the well-known single-crystal behavior: among others, a more complex geometrical structure and quantization of electronic states in the spatially confined systems which also leads to a decrease of energy transport into the substrate. Many of the distinct chemical and catalytic properties are determined by the new morphology of the nanoparticle ensembles, caused by large surface-to-volume ratios and the limited particle size.[7] By varying the preparation conditions, it is therefore possible to tune the system properties toward the demands of a specific chemical reaction. In addition, the special optical characteristics[10,32] of nanosized metal particles have a very strong influence on the photochemistry. All these factors determine the interaction of MNPs with adsorbed molecules and consequently their performance in photochemical reactions.

Table 1. Factors Controlling Photochemistry on Single-Crystal Metals and Supported Metal Nanoparticles (MNPs)

	single-crystal metals	supported MNPs
geometric structure	simple	complex
electronic structure	electron bands	confined states, discrete for smaller NPs
chemical properties	fixed	tunable
optical properties	fresnel: continuous behavior	Mie: resonance behavior
energy transport to the substrate	fast	slow
particle−particle interactions	no	yes

One important consequence of the tunable morphology of particle systems in terms of shape, size, and environment of the MNPs is the possibility to adapt and tailor their optical properties relative to bulk crystals.[10] In particular, new collective modes in electron excitations, which can be described as Mie-type surface plasmon−polaritons, are of utmost importance to drive photochemical reactions. Exploiting the strong field enhancement induced by particle plasmon resonances, the first studies of the photochemistry on MNPs were done in the mid-1980s. Experiments at this time were inspired by the experience and implications derived from surface-enhanced Raman spectroscopy (SERS), which uses the plasmon-induced electromagnetic near field to stimulate optovibrational excitations of adsorbed molecules.[33,34] It is known that the topology of MNP ensembles can be important also for thermally induced catalysis because it influences the transport of chemical species between MNPs and the support (spill-over effect[35]). This should also hold for photochemical reactions and will add to the benefits already present due to the special optical properties of MNP ensembles as determined by their topography and interactions with the support.[10] The full exploitation of the relations between these aspects still needs further research.

While the optical properties of MNPs are of primary importance in the initial photoexcitation process, the transfer of electronic and thermal energy within MNPs as well as between the MNP and the adsorbate and the substrate are decisive, too. This is especially critical for the chemistry induced by ultrashort laser pulses because the conversion and transport processes occurring can determine the lifetimes of electronically excited adsorbate states and therefore the reaction rates, final energy distributions, and branching ratios of chemical products. Electron energy transport at metal surfaces[36,37] and ultrafast surface photochemistry in the subpicosecond regime (surface femtochemistry)[38,39] have been studied since the 1990s using laser-based pump−probe techniques. Also, the ultrafast energy transport at bulk metal surfaces has been characterized in detail.[40−42] However, there are only a small number of studies on energy transport within MNPs in relation to their surface photochemistry.[43]

In fact, the existing literature about actual photochemistry on MNPs is generally very limited; most of the publications concern the photophysics of metal particles. The main topics addressed here are the plasmon field enhancement effect, the plasmon decay and hot electron dynamics, and the influence of particle size and morphology on these phenomena. These aspects are of great importance for our discussion on the subject and will therefore be included in this review. The number of investigations aimed directly at photochemical reactions at MNPs is quite small so far, and consequently, many relevant questions remain open. We therefore believe that an integrated overview, which has not been given so far to the best of our knowledge, is timely and helpful for further development of this field.

This review surveys photochemistry on MNPs, which were prepared in ultrahigh vacuum on well-defined metal or insulator substrates and characterized via common surface science techniques. We will not deal with ultrasmall clusters (number of atoms below about 100) but focus mainly on the diameter range from 2 to 20 nm (some hundred to some 10^5 atoms), and in this sense we use the nomenclature MNPs. However, since most of the existing basic concepts have been developed with embedded particles or particles prepared under less stringent conditions, important work using such samples will also be mentioned where appropriate. We pay special attention to the various differences between bulk metal surfaces and MNPs.

The structure of the review is as follows. In section 2 we give a brief overview of the techniques used and derived properties of well-defined MNPs, stressing those of particular importance to photochemistry. In section 3 we present a general survey of MNP photochemistry and then review the publications which have appeared so far. We provide conclusions and an outlook in section 4.

2. Properties of Metal Nanoparticles

For the study of photochemistry on MNPs, preparation and characterization of the sample are of central importance. Here we summarize the experimental methods for the preparation of MNPs on well-defined substrates and then review their relevant properties for photochemistry, such as geometrical structure and electronic and optical properties, as characterized by means of various surface analytical techniques. Most of the experimental methods are similar to those used for photochemical studies on single-crystal surfaces.[1,44,45] They usually combine classical surface analysis tools and suitable light sources. The main difference between

single-crystal and MNP studies are the distinct preparation techniques for the particle ensembles. Concerning optical properties of MNPs, there are numerous studies which cannot be covered comprehensively in this review.[10,46] In addition, many of the earlier investigations were done on embedded particles; so their results cannot always be transferred easily to UHV-prepared systems, even though many basic concepts were developed there. Here we try to give a survey of what is currently known based on selected papers of both theoretical and experimental studies. We specifically focus on ultrafast electron dynamics within MNPs as this should play a decisive role in photochemistry. We also deal with topics related to plasmonics as we expect that the collective excitations will play a crucial role in surface photochemistry on ensembles of optically coupled MNPs.

2.1. Preparation and Geometric Structure of Metal Nanoparticles on Well-Defined Surfaces

MNPs on well-ordered oxide films have been prepared and analyzed in numerous studies with the aim of fabricating model systems for heterogeneous catalysis.[4−9] Typical substrates are thin oxide films grown on metal supports, such as a two-layer Al_2O_3 film on NiAl(110) and an MgO film on Mo(100). Chemically inert bulk supports such as highly oriented pyrolytic graphite (HOPG) and quartz have also been used. Since the particles usually nucleate at point and line defects,[47] the substrates are ion sputtered in some cases prior to metal deposition in order to produce well-defined binding sites and increase the stability of the particles.[48,49]

Metal atoms are usually deposited from an electron beam evaporator whose flux is calibrated by a quartz crystal microbalance (QCM). By choosing the substrate temperature and defect concentration on the surface, the size and morphology of the MNPs can be controlled. For example, Pd grows at low temperatures (∼100 K) into small amorphous clusters on Al_2O_3/NiAl(110), whereas at room temperature (∼300 K) it forms relatively large and crystalline NPs with dominantly (111) oriented top and side facets and a minority of (100) facets.[50] Gold NPs show a very similar growth behavior to Pd apart from the fact that due to the higher mobility of Au lower temperatures are required to grow particles of similar sizes as for Pd (Au nucleation on Al_2O_3 is a very special case and should not be compared to Pd nucleation[51]).[52] On the other hand, Ag NPs are more difficult to crystallize. Typical cluster densities are on the order of 10^{11} particles per cm^2.

The size distribution of MNPs is normally broad when deposited on oxide surfaces. For MNPs with plasmon resonances in the visible region, such as Ag NPs, the size distribution can be significantly narrowed down by the so-called 'laser shaping' method developed by Träger and coworkers.[47,53] In this method the MNPs are resonantly heated by laser pulses tuned to the plasmon energy so that smaller particles successively evaporate while larger ones decrease their size in the course of the laser treatment. We will review laser heating and morphology changes of MNPs in section 2.3.5. MNPs with mean diameters above 50−100 nm can also be fabricated by lithographic techniques, which allow excellent control over the particle sizes and shapes and their arrangement on the surface.[54,55] Lithographically prepared NPs are, however, above the size range discussed in this review, and particle cleanliness also presents a problem for defined photochemical investigations.

The geometric structures of MNPs can be probed by various techniques, such as scanning tunneling microscopy (STM), atomic force microscopy (AFM), transmission electron microscopy (TEM), and spot profile analysis of low-energy electron diffraction (SPA-LEED). STM and AFM provide local structural information down to the atomic scale. Characteristic STM images of Pd and Ag NPs are shown in Figure 1. SPA-LEED provides information about coverage,

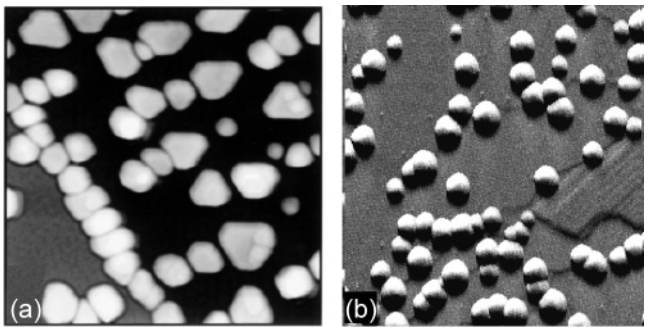

Figure 1. STM images of (a) Pd- and (b) Ag-nanoparticles on Al_2O_3/NiAl(110). Image sizes: 65 nm × 65 nm and 130 nm × 130 nm. Reprinted with permission from (a) ref 50 [http://link.aps.org/abstract/PRL/v83/p4120] and (b) ref 48 [http://link.aps.org/abstract/PRL/v84/p3994]. Copyright (a) 1999 and (b) 2000 The American Physical Society.

particle size, and interparticle distances averaged over a sample area of the diameter of the electron beam (<1 mm, i.e., over approximately 10^9 particles). After correction of tip convolution effects inherently connected to scanning probe techniques, good agreement was obtained between SPA-LEED and STM/AFM results.[56] An additional technique providing atomic resolution is TEM; however, its ex-situ character due to the usual procedure of transferring the sample through air limits its use for characterization of UHV-prepared MNPs. The principles and typical applications of these methods are reviewed in ref 7. For relationships between the structure and (thermal) catalytic activities, readers are referred to ref 7.

2.2. Electronic Properties

The electronic structure of MNPs has considerable implications for their photochemical performance and therefore should to be studied with high accuracy. The electronic properties of MNPs are probed mainly by two methods: photoelectron spectroscopy as a nonlocal technique and scanning tunneling spectroscopy as a local technique. Several variants of either type, possessing a number of advantages and disadvantages for the study of MNPs on surfaces, have been developed so far which are briefly surveyed in the following.

2.2.1. Electronic Structure

The electronic structure changes related to the transition from a single atom to an extended metal crystal are schematically illustrated in Figure 2.[57] X-ray photoelectron spectroscopy (XPS) and ultraviolet photoelectron spectroscopy (UPS) are generally used to probe the electronic structure of MNPs. On one hand, gradual development of metallic bands from single atomic orbitals is observed in the valence band region with increasing cluster size. Additionally, a well-defined Fermi edge develops in clusters containing several thousands of atoms, which separates occupied and unoccupied electronic states. The metallic properties appear at about 1 nm, and a bulk-like band structure is

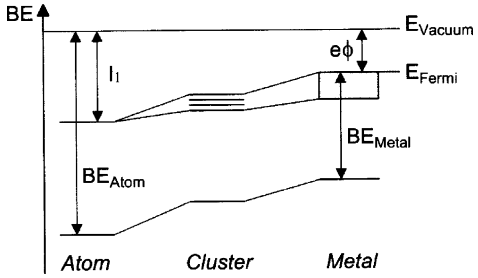

Figure 2. Diagram illustrating the evolution of electronic states from an atom to a metal. Reprinted with permission from ref 8. Copyright 1999 Elsevier.

formed at about 3 nm in diameter.[58] On the other hand, characteristic shifts of the binding energy (BE) of core and valence electrons are detected.

The shifts comprise chemical (initial state) and incomplete-screening (final state) effects[59] occurring as a result of the limited cluster size. The latter influence on the photoemission is not present in extended metallic systems and reflects the different screening and delocalization behavior of the positive charge left on the aggregate during and/or after electron emission. The final state effect results in a shift of the entire PE spectrum according to the Coulomb energy between the localized charge on the cluster and the photoelectron and is therefore proportional to the reciprocal particle diameter.[57,60,61] Recently, lattice strain in the MNPs has been discussed as a reason for BE shifts.[62]

The UPS/XPS data are also useful to estimate the role of electronic coupling between the metal substrate supporting the oxide film and the MNP.[7] For example, for Pd and Rh deposits on thin alumina films on NiAl(110), the effect of charge transfer from the substrate was negligible on the time scale of the core ionization process (10^{-17} to 10^{-15} s, depending on type and mode of excitation).[5,63] Moreover, a comparison of Auger and autoionization spectra of CO-covered Pd particles revealed that even on the time scale of the core hole lifetime (some 10^{-15} s) no detectable charge transfer occurs.[64] As schematically summarized in Figure 3, electron tunneling from the NiAl substrate can thus be safely disregarded in the analysis of sufficiently fast perturbations in the electronic structure of metal deposits, such as creation of core holes. On the other hand, charge transport through the thin oxide is fast enough to prevent permanent charging of the MNPs. It is important to note that these conclusions drawn for ultrathin Al_2O_3 films are not necessarily correct for all thin-film supports and metal−oxide film combinations and must be checked for each case.[65]

Final state effects can also become important for spectroscopy in the valence band region because of the influence of the finite escape time of the photoelectron and the slow neutralization from the substrate (dynamic final state). Recent UPS data of Ag NPs on HOPG have been interpreted in this scheme by Hövel and co-workers.[66,67] The dynamic final state effect is also seen for core level emission of Au NPs on $TiO_2(110)$[68] as well as for valence and core levels of ligand-protected Ag and Au NPs on HOPG, respectively.[69,70] Since the dynamic final state effect involves states near the Fermi level and therefore reflects the MNP−substrate interaction, it might contain some information about its influence on the photochemistry of adsorbates on MNPs. However, further investigations are necessary in the field.

Electronic states of single MNPs have been observed by scanning tunneling spectroscopy (STS). STS is a special operation mode of STM where the tunneling current I is measured as a function of bias voltage V at a fixed tip location above the surface. The differential conductance (dI/dV) gives information on the local density of states in the sample surface, assuming a sufficiently unstructured DOS of the tip. Due to its high lateral resolution, STS is a powerful tool to investigate the electronic properties of single nanostructures around the Fermi level[71] as well as local electron transport properties.[72] Quantized electronic states have been observed in small Ag and Au clusters as well as on the surface of larger Au NPs on HOPG.[73,74]

Figure 4 shows confined Shockley surface states on top of the Au NPs on HOPG.[74,75] Ag NPs on thin alumina films on NiAl(110)[76] and ligand-stabilized Pd NPs on Au(111) films also showed the presence of localized electronic resonances in dI/dV spectra.[77]

2.2.2. Electron Dynamics

The dynamics of the hot electrons photogenerated in the MNPs can play a crucial role in determining the dynamics of chemical reactions on their surfaces if these hot electrons trigger the chemical processes in the adsorbates. We therefore briefly review the knowledge existing on these processes.

The time sequence of photoexcitation and relaxation of electrons in a MNP can be classified into several steps.

Step 1: Absorption of a photon excites an electron below the Fermi level of a MNP and produces an electron−hole (e−h) pair.

Step 2: This creates a transient athermal e−h distribution, which develops rapidly by electron−electron scattering, shifts down in energy, and broadens. The time scale of these processes strongly depends on the hot electron energy, being very fast (below 10 fs) at high energies (2−3 eV) with respect to the Fermi level and becoming slower (tens of femtoseconds) with decreasing energy. In bulk crystals or thick films this relation can be approximated by Fermi liquid theory.[78]

Step 3: On a time scale from some 100 fs to 1 ps a quasithermal distribution describable by a distinct electron

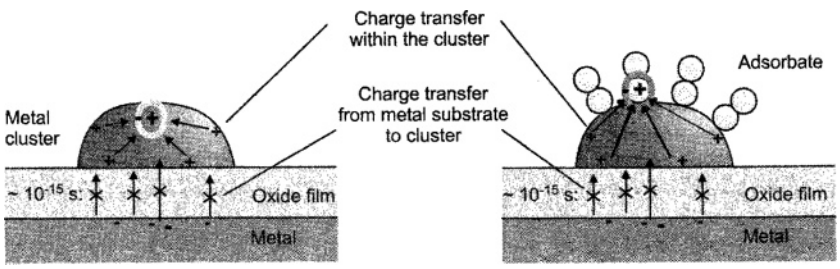

Figure 3. Illustration of the screening mechanisms after creation of a core hole within a cluster (left) and within an adsorbate layer (right). Charge-transfer screening provided by the metal underneath the oxide is not observed during the core hole lifetime for the former. Reprinted with permission from ref 8. Copyright 1999 Elsevier.

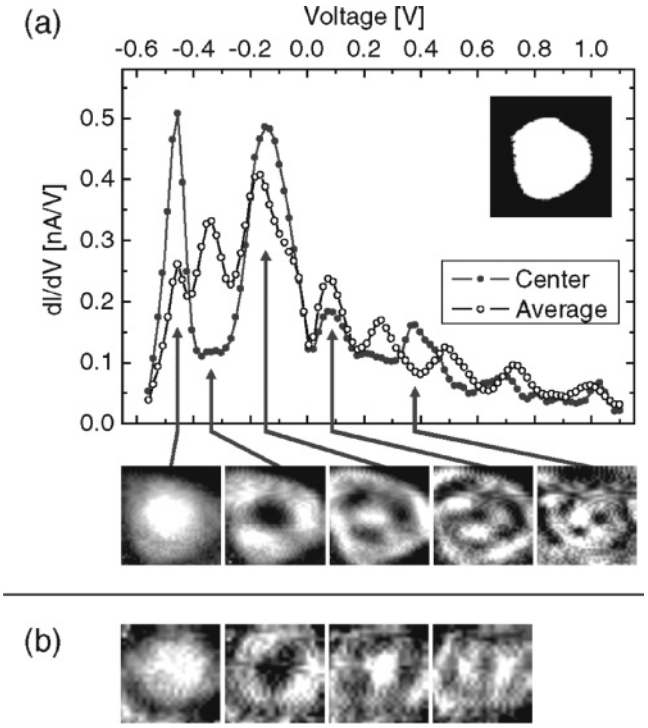

Figure 4. (a) Scanning tunneling spectra measured on the (111) top facet of a gold nanoparticle (area of the (111) top facet: $\Omega = 37$ nm^2, height $h = 3.9$ nm). (Top) dI/dV spectra measured in the center of the facet (full dots) and averaged over the total facet area (open dots). The facet shape is shown in the inset [(10×10) nm^2]. (Bottom) dI/dV maps [(4.5×4.5) nm^2] for five different voltages corresponding to the energy positions shown. (b) dI/dV maps [(5×5) nm^2] for a second nanoparticle with $\Omega = 47$ nm^2 and $h = 2.5$ nm measured at four different voltages. Reprinted with permission from ref 74 (http://link.aps.org/abstract/PRL/v90/p166801). Copyright 2003 The American Physical Society.

temperature is reached, which is much higher than the lattice temperature.

Step 4: The obtained thermal hot electron distribution cools down further by electron−phonon interactions, which is an even slower process occurring on a time scale of several to some hundred picoseconds or longer. In this state the two temperature model[79] applies.

After step 1 the subsequent steps overlap in time scale; they proceed in a correlated way. As we will discuss below (section 3.1), these intermixing processes can be important for surface photochemistry on MNPs. These relaxation mechanisms of hot electrons in embedded MNPs have been studied by subpicosecond pump−probe experiments and theory.[58,80]

Effects on e−e scattering at the surface of Ag NP's have been studied theoretically in terms of screening of the mobile s electrons by the localized d electrons.[81] Experimentally, femtosecond pump−probe studies on Ag NPs showed that electron thermalization due to electron−electron interactions in Ag NPs is faster[80,82,83] than or close to[84] that in the bulk. No dependence on the environment (matrix) and sample preparation was found there, whereas the e−e interaction increased sharply with decreasing size ($R < 5$ nm). Here the size dependence was explained by the reduced screening of the e−e Coulomb interactions at the surface for smaller particles.[58]

On the other hand, electron confinement could act oppositely on e−e scattering, since the wave functions of the hot electrons should become standing wave states with reduced interactions at the boundaries as already argued very early.[85] In a classical picture these correspond to closed-loop scattering (ref 10, p 81). In principle, electron−electron scattering should then decrease with decreasing size of the particle. It has been argued[58] that this effect is not important for metals because of their large electron density.

Electron−electron scattering effects within small particles will be counteracted by scattering at surface irregularities and defects as well as at adsorbate layers (see CID, section 2.3.4). We want to point out that the contributions of such interface states could change when the particle size changes, even if all preparation parameters are kept constant.

Very recently, Quijada et al.[86] investigated the lifetimes of excited electrons in MNPs theoretically. Using DFT on a jellium model for spherical particles of a few nanometer sizes, they showed that the two influences, (1) the decreased density of states and (2) the reduced screening in MNPs relative to bulk materials, can counteract and largely cancel each other. An important result is that Fermi liquid behavior is definitely not expected. Since both influences depend on particle size and electron energy, oscillatory dependences can result for small particles. For larger particles, i.e., in our range, they approach a limit which is still energy dependent but only weakly changes with size: They arrived at a lifetime of ~5 fs for electrons of 1 eV, which is on the same order of magnitude as for the respective bulk material. Only at very small sizes (<2 nm), was an oscillatory behavior between 4 and 30 fs observed and traced back to the discretization of cluster levels and their variable filling. Generally, it appears that the differences of electron−electron scattering between bulk and reasonably large MNPs ($d > 2$ nm) of the same material are not drastic compared to changes when going from one material to another as long as no surface irregularities or defect states are taken into consideration. In reality, however, the behavior could be dominated by such defect contributions, leading to elastic as well as inelastic scattering events.

For bulk metal substrates these hot electron dynamics have been studied extensively by both theory and 2PPE experiments[42,87,88] and are reviewed in the review by Wolf in this special issue of *Chemical Reviews*. Equivalent experiments for MNPs are still scarce, although there are studies for silver and gold NPs on HOPG using 2PPE by Pfeiffer and coworkers.[89,90] On the other hand, electron dynamics in MNPs embedded in a matrix or supported on a solid substrate have been studied by optical spectroscopy methods and theory.[58,91] There appears to be disagreement about the changes in hot electron cooling times induced by the finite particle size, i.e., by the fact that the particle diameter is smaller than the electron mean free path.[10] (It should be realized that in our size range all typical attenuation lengths as well as the photon wavelength are much larger than the particle diameter.) The main argument given[58] is that the surface provides additional scattering centers (surface states, defects, irregularities), so for mean bulk scattering lengths exceeding the diameter of the particle, the scattering should increase with the surface/volume ratio for decreasing size, i.e., it should scale with $1/R$. Indeed, this result has been obtained in various theoretical investigations.[10]

In a recent publication (ref 105) which pertains to the electron−electron interactions at energies between the maximum intermediate state energy and 1.5 eV above the Fermi level, i.e., in the range of decisive importance for electron-

transfer-mediated photochemistry, the (strongly energy dependent) electron lifetimes are increased in Ag MNPs compared to a massive Ag film (see Figure 5[92−94]). The

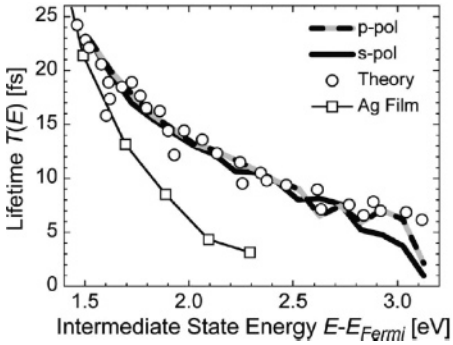

Figure 5. Results for Ag nanoparticles on graphite for the inelastic electron lifetime $T(E)$ as a function of the intermediate state energy above the Fermi level, E_{Fermi}. The two different datasets were acquired with p-polarized and s-polarized excitation. Theoretical predictions (ref 92) and experimental results for a 15 nm thick Ag film (ref 93) are shown for comparison. Reprinted with permission from ref 105 (http://link.aps.org/abstract/PRB/v70/p193401). Copyright 2004 The American Physical Society

shapes of the energy dependences are again in acceptable agreement with Fermi liquid theory. More results for carefully prepared clusters will be necessary to disentangle these possible contributions.

Regardless of the detailed mechanism of e−e and e−h scattering it is clear that the electron temperature rise after electronic thermalization (step 3) in MNPs can be much higher than in bulk metals due to limited sizes and confinement effects. The calculated maximum electron temperature rise as a function of the particle size is presented in Figure 6. For very small MNPs ($R < 2$ nm) the electron temperature

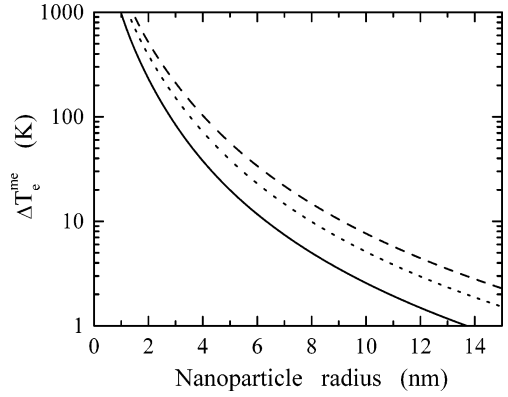

Figure 6. Maximum equivalent electron temperature rise ΔT^{me}_e induced by absorption of one (full line), two (dotted line), and three (dashed line) near-infrared photons (1.3 eV) in a spherical silver particle as a function of its radius. Reprinted with permission from ref 58. Copyright 2001 American Chemical Society.

rise amounts to several hundred Kelvin even by single infrared photon absorption.

It should also be noted that the dynamics (steps 3 and 4) depends on the excitation density. In Figure 7 the time evolutions of the electron temperature are compared for low and high photon fluences. The decay becomes slower and nonexponential as the excitation density is increased. In the presence of plasmon excitations in Ag NPs, for example, which will be dealt with in detail in section 2.3, it is conceivable that a very high excitation density can be easily

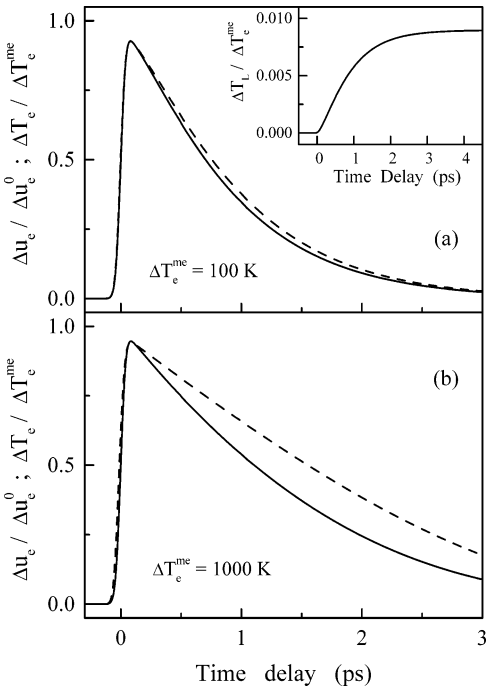

Figure 7. Normalized time dependence of the electron excess energy, Δu_e(full line), for electron excitation with a 25 fs pump pulse and $\Delta T^{me}_e = 100$ (a) and 1000 K (b). Δu°_e is the total energy absorbed by the electrons. The dashed lines show the correlated electron temperature rise. (inset) Corresponding time dependence of the normalized lattice temperature. Reprinted with permission from ref 58. Copyright 2001 American Chemical Society.

achieved if the photon energy matches the plasmon resonance, resulting in electric field enhancement and increased e−h pair creation due to plasmon decay (Landau damping). When photon emission as the main relaxation mode of plasmons can be excluded as for particles smaller than 10 nm,[10] most of the electron energy is eventually converted to the heat of the lattice due to electron−phonon interactions.

Zhdanov and Kasemo recently gave an analysis of the sequence of relaxation processes of hot electrons as related to photochemistry at MNP.[43] They pointed out that one has to distinguish between a low excitation regime where the above considerations appear to be applicable and a regime of high excitation density in which the electron temperature cools much more slowly because of confinement effects.

Under the high excitation densities, thermal processes of adsorbed molecules on MNPs can be comparable to or dominant over the photochemical processes. It is therefore an important issue for photochemistry on MNPs to distinguish photochemical processes from thermal processes. Heating of MNPs as well as of bulk metals by short laser pulses has been studied in some detail. We will come back to this point in section 2.3.5.

2.3. Optical Properties

The optical characteristics of MNPs are the consequence of their distinct electronic and geometric properties and of particular relevance for surface photochemistry. They have been studied extensively. Earlier research has been reviewed in the monumental work by Kreibig and Vollmer in 1995.[10] More recent studies are found in ref 46. The main concerns here are the dependences of absorption spectra of MNPs on their sizes and shapes, particle−particle interactions, and their environments. A large number of data are available for

supported and embedded particles of alkalis, Ag, and Au, which formed the basis to establish most of the mentioned aspects (see ref 10). Additional details became known more recently using time-resolved laser spectroscopy. Here we point out some aspects of the data which are of importance for photochemistry.

2.3.1. Plasmon Field Enhancement

One of the outstanding phenomena in the optical response of MNPs is the size- and shape-dependent collective electronic excitation called Mie plasmon.[10] It leads to strong field enhancement around the particles which is decisively important in surface-enhanced Raman spectroscopy (SERS). It is responsible for a large increase of absorption seen in all photoinduced effects. Practically, the exceptionally strong plasmon modes in Ag and Au NPs have been exploited since the Middle Ages to produce the intense colors in stained glass. They have been scientifically explored since Faraday,[95] mainly in the condensed phase. This excitation is also used in various types of sensors for medical and biological purposes[32] where, in addition to field enhancement, the sensitivity of the plasmon to changes of the dielectric functions of the material surrounding the MNPs is exploited. Both effects are also expected to play a role in MNP photochemistry. In fact, the field enhancement motivated the earliest study of plasmon effects on surface photochemistry (section 3.2).

2.3.2. Plasmon Lifetime and Decay

The plasmon damping mentioned above can proceed by a number of mechanisms, in particular Landau damping, photon emission, electron−hole pair production, surface scattering, and chemical interface damping (see section 2.3.4). The dependence of plasmon decay processes on the particle size can be summarized as follows.[96] For large MNPs with $R > 10$ nm, radiation damping is the main factor limiting the plasmon lifetime. At small sizes ($0.5 \leq R < 2$ nm), the decay into electron−hole pairs (Landau damping) dominates. For intermediate sizes, both effects compete. Most of these mechanisms will also be active following nonresonant photon absorption. If strong contributions of photon emission as the main relaxation process of the plasmons can be excluded, the first product of plasmon decay is very hot electron−hole (e−h) pairs which in nonresonant excitations will be the direct product. The temporal sequences occurring by and after the decay of plasmon excitations are of potential importance for surface photochemistry on MNPs.

The plasmon lifetimes, mostly derived from resonance widths and hole-burning experiments, have been found to be very short. Plasmon dephasing in Na clusters on a LiF substrate has been measured as $\leq$15 fs by femtosecond time-resolved second-harmonic generation.[97] For Ag NPs on quartz and sapphire surfaces the width depends on size, shape, and chemical environment (e.g., adsorbates and support), as observed by employing a combination of persistent spectral hole burning and laser shaping.[98] The influence of the substrate has also been studied by reflectivity measurements and determined via excitation of multipolar plasmon modes for Ag NPs on α-Al_2O_3(0001).[99] Absorption spectra of individual Au NPs with diameters down to 5 nm have recently been measured by a photothermal heterodyne imaging method.[100] Intrinsic size effects were observed as a broadening of the surface plasmon resonance; these data can be compared to those from the photon-STM described in the next section. Pfeiffer and co-workers investigated in detail the dynamics and typical decay times of plasmon excitations in Ag NPs on HOPG[89,90,101−105] and again found values of a few femtoseconds. Plasmon enhancements in the 2PPE (see below) yield were observed for Au NPs on HOPG[106] and Ag NPs on Si(111)[107] and on thin alumina films.[108] In the latter case, the size dependence of the 2PPE yield was studied explicitly, and possible effects on photochemistry were discussed.

With these decay processes of plasmons in mind, we review the experimental studies related to MNP plasmons by 2PPE, PEEM, photon-STM, and cathodoluminescence.

Two-photon photoelectron spectroscopy (2PPE)[37,38,109−113] is widely employed to study surface states and image states on metal substrates as well as unoccupied states localized on substrates and adsorbates. In a pump−probe regime the lifetimes of excited states also become accessible to the experiment. Application of 2PPE to explore MNPs was first reported in 1999. Wöste and co-workers studied the size dependence of spectral shapes and lifetimes for small silver clusters containing 2−9 atoms on HOPG.[114] They found a pronounced odd/even effect in the photoelectron spectra and an increase of the lifetime of the cluster anions with size. Ertel et al. studied the 2PPE of Ag NPs (~5 nm) on HOPG.[101] They found an enhancement of the photoemission yield by a factor of 50 for laser energies above $h\nu = 3.1$ eV and attributed this to involvement of plasmon excitations in the photoemission process (see below). A prolonged relaxation time (up to 2 ps) of intermediate hot electron states was detected in time-resolved two-color 2PPE measurements of this system.

2PPE is especially useful to study the effects related to plasmon excitations in silver and gold NPs because their resonance energies (UV−vis) are close to photon energies of typical ultrafast laser systems. Figure 8 shows the photon energy dependence of the 2PPE yield from Ag MNPs on

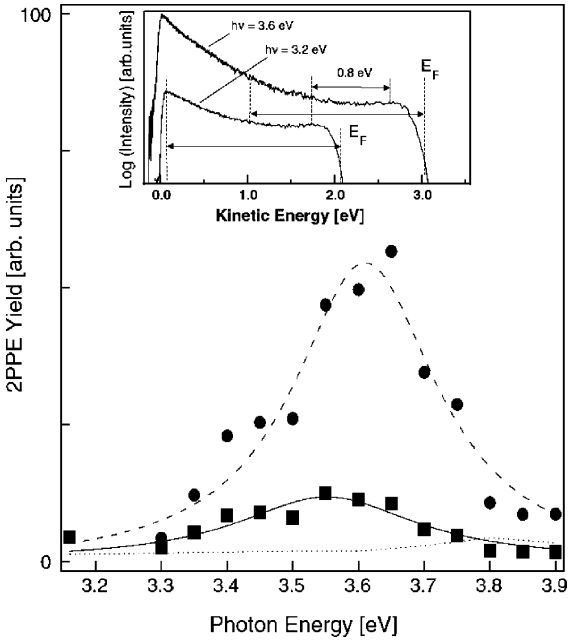

Figure 8. Photon energy dependence of the 2PPE yield of Ag nanoparticles. The solid circles and solid squares represent total and partial integrations over the 2PPE yield, respectively. The solid and dashed curves indicate Lorentzian fits. The dotted curve shows the total 2PPE yield of Ag(111). (inset) 2PPE spectra of Ag nanoparticles of approximately 10 nm diameter at $h\nu = 3.2$ and 3.6 eV. The arrows indicate the width of integration and peak shift. Reprinted with permission from ref 108. Copyright 2005 Elsevier.

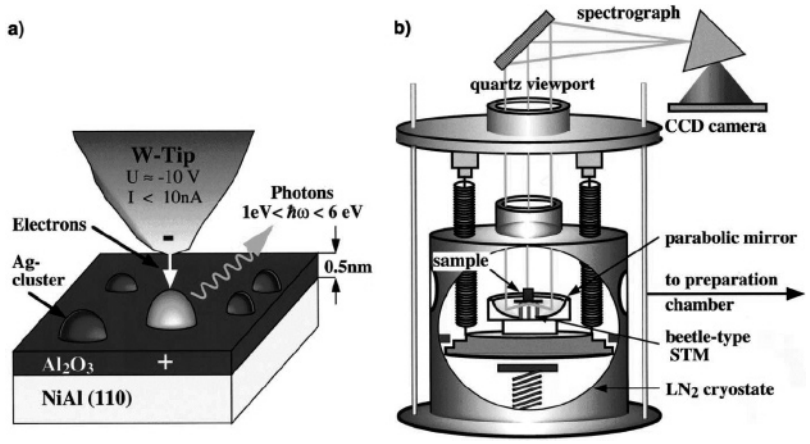

Figure 9. Experimental setup for photon emission spectroscopy of single Ag nanoparticles supported on thin alumina film (0.5 nm) in STM. (a) Schematic drawing illustrating the cavity below the tungsten tunnel tip. Electrons with given parameters (tunnel voltage, current) are field emitted from the tip into an individual Ag nanoparticle; subsequently, emitted photons are detected in the energy range between 1 and 6 eV. (b) The analysis part of the experimental setup consists of a beetle-type STM (tip direction upward) housed in a UHV chamber, combined with a grating spectrograph and a CCD camera in air. The sample is prepared and characterized in a second chamber and can be moved into the UHV chamber using a transfer rod. Reprinted with permission from ref 119. Copyright 2001 Elsevier.

Al_2O_3/NiAl(110) which exhibits resonant behavior at 3.6 eV. In the inset, 2PPE spectra at 3.2 and 3.6 eV are compared.[108] Information on the dynamic response is attainable if such measurements are carried out in a time-resolved mode.

Photoelectron emission microscopy (PEEM) is a potentially powerful tool for the study of MNPs. Although its spatial resolution is limited to about 20 nm at present, it combines a number of advantages. The imaging is much faster compared to the scanning probe techniques STM and AFM, rendering time-resolved measurements possible. It can be combined with photoelectron spectroscopy by choosing proper light sources to yield spectroscopic information and can be performed in a pump−probe mode to explore unoccupied states. Cinchetti et al. observed two-photon photoemission (2PPE) images of Ag NPs ($R \geq 20$ nm) and silver films on Si(111) by a PEEM combined with a time-of-flight photoelectron spectrometer and pumped by a femtosecond laser (∼200 fs).[107] They observed a significant increase of the photoelectron yield by up to 160 times on the particle-covered areas with respect to the flat Ag films, although individual NPs were not resolved. A time resolution as short as 50 as was attained very recently by Petek and co-workers[115] in their time-resolved PEEM experiments on silver grating structures. A time-resolved version of a 2PPE-PEEM with higher spatial resolution should be the ultimate technique for the study of electron dynamics of MNPs. In this context it is important to note that the lateral resolution of an aberration-corrected PEEM called SMART is approaching the theoretical resolution limit of 5 nm.[116]

The spectral response of an ensemble of MNPs can be measured by exciting an extended sample area by the low-energy electron beam from a distant source (cathodoluminescence). Compared to optical extinction spectroscopy, which probes the allowed electric dipole transitions, stimulation by electron impact also provides information on possible excitation channels not directly accessible by optical transitions. Cathodoluminescence was, for instance, employed to study the radiative deexcitation of Mie plasmons in Ag NPs on a thin alumina film on NiAl(110).[117] From analysis of these spectra it was concluded that the optical coupling between silver MNPs was of minor importance at island densities below $\sim 10^{11}$ cm^{-2}. Spectral changes after annealing of the sample were also monitored and attributed to modifications in the shape and size of silver MNPs during annealing (Ostwald ripening and increasing aspect ratio).

Luminescence from individual MNPs can be studied by combining light emission spectroscopy and STM, a method called 'photon-STM'.[48,118] In this technique the photon emission is stimulated by injection of field-emitted electrons from the STM tip used as local electron emitter into single supported particles. Emitted photons are collected by a parabolic mirror surrounding the STM head, steered by optics through a quartz view port of the vacuum chamber, focused onto the slit of a UV−vis-grating spectrograph, and detected with a liquid nitrogen-cooled CCD camera (Figure 9). This setup enables simultaneous imaging and spectroscopic analysis of single particles on solid surfaces. Plasmon excitations in Ag and Au NPs have been studied on alumina and titania supports by Nilius et al.[48,119−123] The experiments on Ag/Al_2O_3/NiAl(110) focused on the dependence of the plasmon excitations on the particle size (Figure 10).[48,119] For

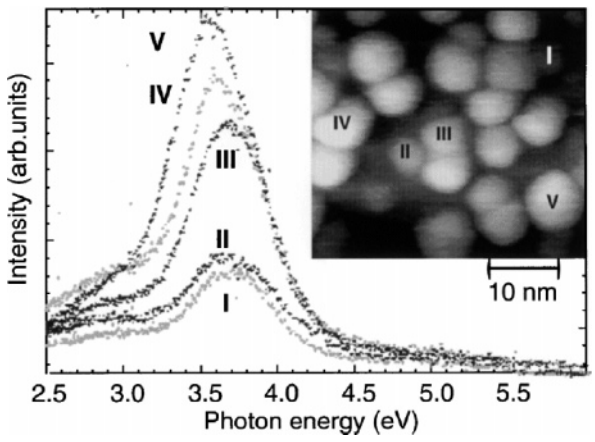

Figure 10. Photon emission spectra of differently sized Ag nanoparticles. The inset shows the corresponding STM image. Reprinted with permission from ref 48 (http://link.aps.org/abstract/PRL/v84/p3994). Copyright 2000 The American Physical Society.

Au NPs on thin alumina films as well as on bulk TiO_2 the electromagnetic coupling between plasmons and electronic excitations in the substrate was discussed. From the observed broadening of the plasmon peaks a reduction of the plasmon

lifetime was suggested for thin film supports with respect to bulk oxides.[120] Shifts of plasmon energies between 300 and 500 nm were observed for single Ag−Au alloy particles,[122] which might be exploited for selective photochemistry by tuning the plasmon resonance to the demands of the reaction process.

The electromagnetic coupling between neighboring NPs has been studied by fabricating particle ensembles with varying number densities and investigating their optical response.[124] With decreasing particle−particle distance, an increase in the plasmon energy has been observed and assigned to a destructive coupling of out-of-plane plasmon modes. The coupling between MNPs in close proximity has also been studied theoretically because of its outstanding importance for photonic crystals and single-molecule detection in surface-enhanced Raman spectroscopy.[125] We will come back to this below. The role of particle−particle interactions in the photochemistry of complex MNP systems has not been explored yet, although a considerable influence is expected especially for high particle densities (see also section 2.3.3). The dependence of the photon emission signals on the long-range order in nanoparticle ensembles has been demonstrated by photon-STM experiments on self-assembled layers of ligand-stabilized silver particles on HOPG.[126] It should be mentioned in this context that near-field spectra of single gold MNPs have recently been observed by a scanning near-field optical microscope (SNOM).[127] This method is potentially interesting as it allows not only detection of optical signals but also controlled stimulation of a photochemical reaction on a single MNP.

Concerning the transfer of excitations from the MNP to the substrate, our knowledge is based on experiments that have been performed in a photon-STM by exciting Ag NPs supported on TiO_2 single-crystal surfaces of varying bulk conductivities. For Ag NPs on weakly reduced TiO_2, radiative decay of Mie plasmons shifting to higher energies with decreasing particle size was observed, while on strongly reduced TiO_2, plasmons were dissipated to e−h pairs in the oxide and emission spectra revealed radiating decay of TiO_2 excitons.[121] Such observations suggest the possibility of using MNPs as antenna to locally inject e−h pairs into the substrate, on which photochemical processes could then occur. It may even be possible to probe how far away from the point of energy-transfer chemical reactions induced by e−h pairs in the substrate can occur.

2.3.3. Plasmonic Coupling

At the Mie plasmon resonance the polarization of a MNP oscillates at the frequency of the incoming light. This results in the emission of light propagating to infinite distance. In addition, strong near-field light localized in close proximity to the metal sphere is generated. The decay length of the latter is about the diameter of the sphere. As mentioned before, the strongly enhanced fields in and around MNPs at their plasmon resonance can couple in ensembles of such particles. This can lead to drastic effects. A dramatic increase of the optical near-field strength in their surroundings is expected, while field enhancement does not occur in areas with unfavorable geometry. The effect is well known from surface-enhanced Raman spectroscopy (SERS) performed on rough silver surfaces, where only a small percentage of the adsorbed molecules (0.01%) contribute to the total Raman signal as they are localized in areas with extremely high electromagnetic field strengths. Estimations of the Raman cross section yielded field enhancement factors on the order of 10^5−10^7 in such 'hot spots' with respect to the incident field; recently, even higher enhancements up to a factor of 10^{15} (single-molecule SERS) have been claimed.[128,129]

In a series of papers Stockman and his group have shown that plasmonic coupling can lead to a very inhomogeneous field distribution in both space and time which has been described as hotspot formation.[130,131] A prerequisite of the effect is an inhomogeneous distribution of MNPs over the surface with a fractal ensemble being most efficient. While the effect exists even for longer excitation pulses, the most dramatic effects become noticeable for excitation with femtosecond pulses. The calculations were done with simplifying assumptions such as constant phase of the incoming field, dipole−dipole interactions, validity of Mie theory but taking retardation into account by use of the retarded Green's function formalism. They show dramatic localization and increase of the electromagnetic field at distinct spots of the surface, which occur on time scales of a few 10 fs after interaction with a femtosecond laser pulse. While the field distributions are rather homogeneous shortly after arrival of the laser pulse on the sample surface due to the constant phase, inhomogeneous resonance conditions develop within 50−100 fs in different parts of the fractal ensemble and lead to a concentration of the electromagnetic field into nanometer-sized spots. In these hot spots the local field strength reaches values which are 2 orders of magnitude higher than the incident field strength. Additionally, the decay time of the excitation amounts to 100−200 fs, whereas isolated metal particles show plasmon lifetimes of the order of 10 fs or less, as mentioned above. In a very recent paper the applicability of this theory to interpret PEEM experimental data is discussed.[132]

Recently, the study of plasmonic coupling in nanometer-sized photonic devices has been receiving much interest as a new research field called plasmonics.[133−136] It covers a wide range of topics in the fabrication of plasmonic crystals, plasmonic waveguides, plasmonic lithography, perfect lenses with metal slabs, etc. For chemical applications, energy transport from donor to acceptor molecules through thin metal films up to 120 nm has recently been reported.[137] Of course, plasmon excitation has been exploited before the emergence of plasmonics; there have been numerous studies about SERS[128,129] and biosensors.[32] Importantly, hot spots or hot sites[138−140] play a major role in SERS (see above).

Since hot spots at junctions between MNPs appear randomly in the usual samples, design and construction of these sites, so-called hot site engineering, have been attempted by using electron beam lithography (EBL). Plasmonic interactions have been observed for disk-shaped Au NPs[141,142] and Ag NPs[143] ($d \geq 30$ nm) with controlled diameters and interparticle distances made by this method. However, an electric field enhancement has not been observed. This suggests that interparticle distances should be further reduced to achieve observable field enhancement. To date, it has been difficult to produce controlled interparticle distances below 20−30 nm with EBL.[143]

The localization and magnification of electromagnetic near fields in particle ensembles can have an immense impact on photochemical reactions occurring under such conditions. Fabrication of plasmonic nanostructures may also help to control and understand photochemistry on such systems. Following such lines is certainly promising for the future.

2.3.4. Chemical Interface Damping

Damping of plasmons by the surrounding material has long been discussed under the heading chemical interface damping (CID).[98,144−151] It should be important for photochemistry on MNPs which necessarily proceeds in the presence of adsorbed material. CID describes the changes of the energetic position, strength, and lifetime of the plasmon resonance by a surrounding medium, here the adsorbed species. Since it is macroscopically connected with the change of the effective dielectric constant of the medium surrounding the MNP, it has been extensively considered for embedded MNPs.[10] For adsorbates the additional damping effect has been connected to the scattering of hot electrons through unoccupied adsorbate levels;[145,149,150] so, it has to depend on the nature of the adsorbates.

For the interpretation of experimental studies of CID a number of adsorbate-induced effects have been considered, such as changes of the dielectric environment of the particle, oxidation effects reducing the size of the metallic core, and modifications in the particle electron density. Träger and coworkers[146,148] studied the CID of Na and K on 20−40 nm Ag NPs deposited on a LiF(100) surface by optical transmission measurements and changes induced by molecular adsorption. They found strong molecule-dependent effects on energy, width, and strength of the resonance but no size effects. Relatively strong CID for thiol-capped Au NPs has been reported recently.[152]

Very recently retarding effects on the thermalization and cooling of hot electrons in MNPs by adsorbates have been reported by Bauer et al.[153] They found an extraordinarily slow thermalization and cooling for thiolate-covered Au NPs and suggested that these adsorbates work as a reservoir for hot electrons, reemitting them back into the metal conduction band; they termed this negative feedback. Such retarding effects on the thermalization and cooling of the electronic temperature by transient trapping of hot electrons at adsorbates should promote photochemical processes on MNPs by increasing the time and efficiency of interactions between adsorbates and hot electrons if the adsorbates are photochemically active. We stress already here that photochemical processes via transient occupation of LUMOs by excited electrons are directly related to these processes (see section 3.1). Adsorbates will strongly influence the electron dynamics in MNPs and therefore surface photochemical processes on them. Such adsorbate-induced effects on the dynamics have so far not been explicitly considered for photochemistry at bulk metal surfaces.

In addition to the pure chemical effects described above, there may also be influences on the electron dynamics on MNPs (and through them on photochemistry) by the geometrical structure (or morphology) of adsorbates. An influence of the orientation of liquid-crystal coatings on the plasmon splitting of Au NPs has been reported by Park and Stroud.[154]

2.3.5. Laser Heating and Laser Control

For the elucidation of photochemistry on MNPs, it is important to distinguish between nonthermal and thermal processes. In particular, in the presence of plasmon excitations, the electron temperature is expected to be very high due to the increased coupling to light and production of electron−hole pairs by Landau damping ($d \leq 20$ nm). The confinement and electronic isolation of MNPs from the substrate should retard the cooling of the electron temperature resulting in higher probabilities for electron-driven processes. On the other hand, if the thermal conductivity at the interface between MNPs and the substrate is poor (as in the case of MNPs on thick insulating dielectric films), the transient temperature rise can become large enough to induce thermal processes such as desorption and dissociation of adsorbates. Therefore, it is useful to estimate the maximum temperature rise by pulsed laser irradiation at the surface (of MNPs and/or the support) in order to minimize the contribution from thermal processes which might even lead to morphology changes of the MNPs.

The transient *electronic* temperature rise induced by subpicosecond laser pulses can usually be characterized by the two-temperature model[79] or the extended heat-bath model.[42] The electron temperature typically increases by several thousand Kelvin and cools in times on the order of several picoseconds. The transfer to the lattice via coupling to the phonons is slower by a factor 10−100.

Heating of bulk metal surfaces by nanosecond laser pulses has been studied theoretically and experimentally. The peak lattice temperature T_l at the surface (depth $z = 0$) can be calculated by the following formula[155,156]

$$T_l(z=0,t) = T_i + \epsilon(\kappa\rho C\pi)^{-(1/2)} I_0 \int_0^t I(t-\tau)\tau^{-(1/2)}\,\mathrm{d}\tau \quad (1)$$

where T_i is the surface temperature prior to laser irradiation, ϵ is the absorptivity of the surface at the excitation wavelength, κ is the thermal conductivity, ρ is the density, and C is the specific heat. $I(t)$ is the temporal laser pulse shape.

The peak lattice temperature rise by nanosecond laser pulses can be experimentally measured by monitoring the translational energy of molecularly desorbing species (LITD, laser-induced thermal desorption).[157,158] Reasonable agreements have been observed between the calculated temperature $T_l(\max)$ and the peak desorption temperature estimated by the equation[159]

$$T_{des} = ml^2/(4kt_m^2) \quad (2)$$

where m is the mass of the desorbing molecule, l is the flight path length, k is the Boltzmann constant, and t_m is the peak arrival time obtained from the TOF distribution.

On the basis of such calculations, thermal desorption can be distinguished by monitoring the fluence dependence of t_m. However, this is applicable only for molecular desorption. In the case of associative recombination, e.g., $CH_3(a) + H(a) \rightarrow CH_4(g)$,[158] t_m is independent of laser fluence because the kinetic energy gain is determined by the height of the exit barrier of the reaction.

Also, even for true photodesorption, fluence-dependent translational temperatures may be observed in the nonlinear regime. This has been observed, e.g., for O_2 desorption by femtosecond pulses from Pt(111)[160,161] where translational temperatures varying from 600 to 830 K were found. In this case, the contribution of nonthermal processes (DIMET, desorption induced by multiple electronic transitions) has been distinctively confirmed by two-pulse correlation measurements in which a width of 1.7 ps was found, which is much faster than the time scales of surface lattice heating.

Normally, the pulse energies used for LITD experiments are in the range from tens of millijoules to joules, whereas those for photodesorption are on the order of millijoules or lower. Under irradiation with millijoule laser pulses, the

maximum temperature rises are typically below several tens of Kelvin. Therefore, thermal reactions can be excluded if the base substrate temperature is low enough.

A more direct measurement of the transient temperature jump by a nanosecond laser pulse has been conducted by monitoring SHG (second-harmonic generation) from an Ag(110) surface.[162] The validity of the above-mentioned heat-diffusion model was confirmed.

Although the transient temperature jump at surfaces of bulk metals can be well predicted by the heat-diffusion model, that of MNPs has not been established, especially in the presence of the plasmon resonance.

Bourguignon et al. developed a model for the temperature jump induced by a nanosecond laser pulse in MNPs or films on a transparent substrate such as MgO.[163] The model assumes (1) a height of MNPs much smaller than the absorption length of the incoming light and (2) a good thermal contact between MNPs and the substrate. The temperature jump is written as

$$\Delta T = \frac{\Theta A F}{[C(Dt)^{(1/2)}]} \tag{3}$$

where A is the fraction of the beam absorbed by the MNPs, F is the laser fluence, D and C are the heat diffusion coefficient and the heat capacity of the substrate, respectively, and Θ is the coverage of MNPs. This formula allows calculation of the temperature rise of the substrate covered with a thin layer of light-absorbing material. Therefore, it does not predict the temperature rise of MNPs if the thermal contact with the substrate is poor or the thermal diffusion into the substrate is slow. Stietz constructed a more detailed model which takes into account the heat transfer through the particle−substrate contact area with a thermal resistance from a reference as well as heating by the substrate absorption and neighboring particles.[47] This model was used to simulate laser ablation processes for size manipulation of Ag NPs by nanosecond lasers (laser shaping, see below) as mentioned in section 2.1. The typical laser fluences used in laser shaping are several hundreds of millijoules.

Unfortunately, to our knowledge, there are no models which can be useful to predict the temperature jump by laser irradiation in the millijoule or submillijoule range typical for photochemical experiments. However, it is possible to roughly estimate the temperature rise by examining the experimental data.

Träger and co-workers reported time-of-flight distributions of Na dimers desorbed by laser (532 nm) heating of Na NPs on a quartz substrate.[164,165] They estimated the temperature increase from the peak times in the distributions. By plotting the temperature increase as a function of laser fluence, they obtained a slope of 49 K cm^{-2} mJ^{-1} for Na NPs as prepared and of 27 K cm^{-2} mJ^{-1} for annealed NPs.[165] The difference was attributed to the contribution from the absorption at the surface. Using these data it is possible to extrapolate the temperature rise at small laser fluence. This leads, e.g., to a temperature jump of 49 K for 1 mJ/cm^2.

Estimation of temperature jumps may be extremely difficult if there is optical coupling between MNPs as in hot spot sites (see section 2.3.3). Aside from the plasmonic interaction, there may be heat transfer by near-field interaction between two MNPs separated by a submicrometer distance; this coupling has been treated recently, and a model has been suggested.[166] A thermal conductance larger than the contact conductance was found for separations smaller than the particle diameter.

Laser heating of MNPs is utilized to obtain uniform particle size distributions (laser shaping).[47,53,167] A small part of the ensemble of MNPs with specific sizes and shapes (aspect ratios) is heated resonantly in terms of photon energy and polarization by nanosecond laser pulses. A very narrow size distribution (standard deviation in size below 0.13) can be obtained using the plasmon resonance. The narrow size distribution of MNPs obtained by this method was used for measurements of plasmon lifetimes by spectral hole burning.[168,169]

In addition to laser shaping, other methods to control structures,[170] positions,[171,172] and ordering[173] of MNPs on supports are being studied which will be important for more precise control and design of the optical properties of MNPs.

3. Photochemistry on Metal Nanoparticles and Related Studies

3.1. Overview

As outlined in the Introduction, photochemistry on MNPs derives its interest from the changes that can be expected relative to photochemistry on single-crystal surfaces, induced by the peculiar properties of MNPs. To give a basis for discussion it is helpful to briefly summarize the situation on single crystals and then consider the changes to be expected. We summarize the comparison in Figure 11.

To induce photochemistry, i.e., to convert electronic excitation energy into energy of nuclear motion, an optical excitation has to bring the molecule concerned to a potential-energy curve with large slope in the Franck−Condon region, so that the atoms can be accelerated along it. The simplest process usually considered is desorption of an adsorbate or a fragment of it; in a photochemical reaction this may be the starting step. There is a well-established field of knowledge about such processes which is usually termed DIET (desorption induced by electronic transitions, see recent DIET proceedings, refs 174−176). On metal and semiconductor surfaces electronically excited adsorbates are deexcited very rapidly, which strongly modifies the desorption probability compared to dissociation of a similar free molecule. The bond to be broken can be that between adsorbate and substrate or an internal bond of the adsorbed molecule; neutral or charged molecular and atomic fragments can then leave the surface, and fragments can also stay adsorbed.

A number of mechanisms containing various excitation and deexcitation steps have been proposed, of which the oldest is the so-called MGR mechanism.[177,178] At high excitation energies (multiple valence excitations or core excitations; roughly above 40 eV) primary excitations on the adsorbed molecules can be important (see, e.g., ref 179), in particular if they are induced selectively and resonantly.[180] However, at low energies (single valence excitations or even subthreshold excitations in the substrate) the dominant mechanism for photodesorption and reaction usually proceeds via absorption in the substrate and formation of transient negative adsorbate ions by hot electron transfer[1,181] with atom acceleration occurring during their (short) lifetime. This is due to the large penetration depth of photons in this energy range which will lead to high densities of hot electrons of fitting energies. This mechanism can be proved by measuring the dependence of the observed process on the polarization

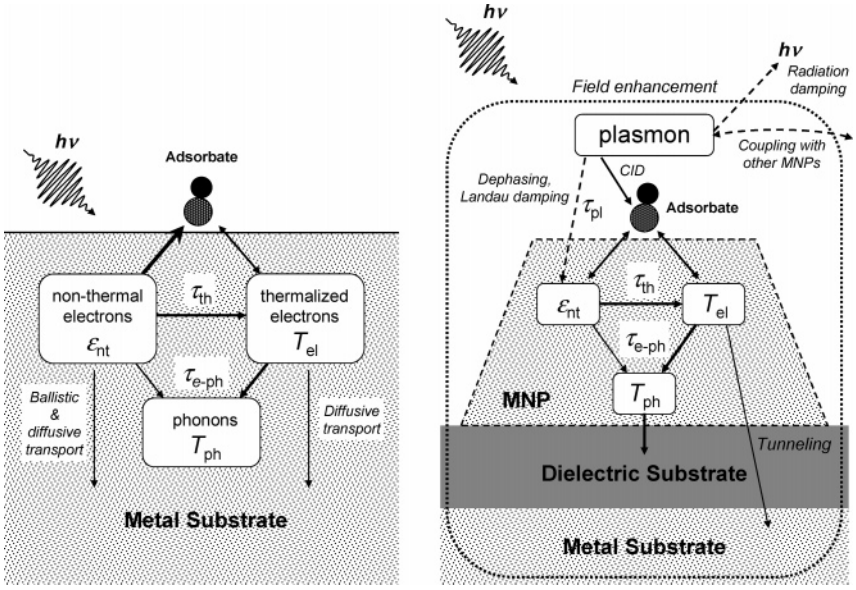

Figure 11. Schematic depiction of the evolution of excitation after photon absorption for a molecule on a single-crystal surface (left) and on a metal nanoparticle (MNP).

of the light—the behavior of bulk absorption is usually distinctly different from that in adsorbate complexes. While the lifetimes of such transient states—with a hot electron localized on an adsorbate unoccupied orbital—will be very small, the frequency of electrons hopping back and forth between substrate and adsorbate is very high. In fact the well-known fast quenching (below 1 fs) of excited molecular states at metal and semiconductor surfaces already contained in the MGR mechanism[177,178] (and recently becoming amenable to direct measurement[182]) is proof of this since this latter process is connected to the hot electron transfer by microscopic reversibility. Again, the induced bond breaking can concern the molecule−surface or an inner-molecular bond. In the latter case the process is similar to dissociative electron attachment[183] (DEA) in molecules which has been investigated in detail by many authors for condensed and adsorbed films.[181,184,185]

A likely sequence of events[42] then is photon absorption in the bulk to produce a highly nonthermal hot electron distribution, cooling of this distribution by electron−electron interactions with its maximum shifting down (time scale in the range of 10−100 fs, with the process slowing down precipitously with decreasing hot electron energy, see Figure 5), and finally arrival at a quasithermal distribution which then couples to the lattice by electron−phonon interactions (time scale some tens or hundreds of picoseconds). If the primary hot electrons match the energy of the molecular negative ion resonance, they can directly be transferred; if this is not the case because most hot electrons start out at too high energy, the second step of redistributing this energy will be the important one since it provides hot electrons with changing and eventually matching energies. The quasithermal distribution will not contain enough electrons with sufficient energy to reach the transient molecular state, at least under low excitation conditions. CID (see above) might be able to channel hot electrons directly into the relevant adsorbate orbitals.

These considerations are applicable only at low excitation densities ($<10^{-4}$ electron/atom).[42] If the latter are beyond the linear range which is likely to occur for very short pulses, nonlinear processes can come into play which have been termed friction-induced desorption[186] and DIMET (desorption induced by multiple electronic transitions).[187,188] The concept of electronic friction in surface processes such as desorption goes back to the 1970s.[189,190] If there is a very large density of excited electrons just above the Fermi level they can convey kinetic energy to the atoms by multiple collisions and lift them across an activation barrier in a friction-like process. Under normal thermal conditions and for laser irradiation with low excitation density such processes are not competitive with phonon-coupled processes; however, they can become important for high densities of (thermalized) hot electrons. As another nonlinear DIET mechanism, DIMET[187,188] was proposed to explain observations of nonlinear electronically induced desorption by short intense laser pulses. This mechanism is essentially a sequential MGR process: even for rapid deexcitation by quenching to the substrate an excitation step can lead to some acceleration of the adsorbate atoms along an excited-state curve. If the next excitation step occurs before the atomic kinetic energy has been dispersed, the effects of recurring excitation−deexcitation cycles can add up leading to bond breaking along that coordinate. In ref 186 the two mechanisms are compared within a unified approach, and it is shown that friction-induced desorption is applicable for cases where the hot electrons have a broad distribution of small energies (e.g., quasithermal) and DIMET occurs for high energies with a comparatively narrow distribution. A critical reexamination has been given by Gadzuk.[40]

If we want to carry over these concepts to MNPs, we have to examine what will change. As discussed in section 2 the main optical effect of MNPs with nanometer size is due to the (material- and size-dependent) existence of the Mie plasmon and the resulting strong enhancement of applied electromagnetic fields. For processes initiated by a primary excitation localized in the adsorbate, this field enhancement will be the main effect. Since the plasmon energies are in the low-energy region as defined above, we expect that for the majority of systems the dominant photochemical mechanism will again be the transfer of hot electrons from the substrate to the adsorbate. These hot electrons are produced in the MNP by plasmon decay in addition to those e−h pairs directly produced by photoexcitation near the Fermi level. There is agreement between the existing reports (see above)

that the lifetime of plasmons is very short, 2−10 fs. It should further decrease due to the CID effect mentioned in section 2.3.4 (see also below). Furthermore, the plasmon constitutes a collective excitation in which the energy of the quasiparticle is distributed over many electrons (in effect all electrons of the MNP), so that it is difficult to see how it could become directly relevant for bond breaking. The main effect of the plasmon for photochemistry is therefore likely the field enhancement and consequent increase of all following events. The only mechanism that can be envisaged to contribute in addition is a friction-type energy transfer to an adsorbate, either directly from the oscillating electrons via Pauli repulsion of the adsorbates or from the large amount of quasithermal electrons after the initial cooling. After its short lifetime the plasmon decays into electron−hole pairs, hot electrons via Landau damping,[191,192] or emitted photons. The first decay path is likely to dominate for our MNPs and will again produce a very athermal hot electron distribution with a maximum energy given by the plasmon energy. The further processes will be as for single crystals but possibly with changed parameters. As discussed in section 2.2.2 there is disagreement as to whether electron−electron scattering is stronger or weaker in MNPs compared to the same bulk material. The most recent results[105] on the scattering of very hot electrons (i.e., those fitting for transient transfer into adsorbate negative ion resonances) indicate a decrease of scattering in MNPs compared to the bulk (Figure 11). This should increase the efficiency for bond breaking. We note that the chemical interface damping (CID) postulated as plasmon damping mechanism by adsorbates (section 2.3.4), i.e., dephasing and energy redistribution by hot electron scattering through adsorbate resonances, is exactly the same process postulated here as the main desorption mechanism. The partial quenching of the plasmon resonance by CID implies that the excitation can be channeled directly into the molecular resonance. This may explain why the effect of plasmon enhancement survives adsorption despite the partial quenching of the resonance it causes. An investigation of this concept appears promising.

An effect which is present in MNPs even outside the plasmon resonance is that of confinement of the excited electron−hole (e−h) pairs by the limited size of the MNP. It has been shown[42] that for a bulk material (here Ru) the ballistic e−h transport into the volume leads to much smaller electron temperatures than expected. If this transport is eliminated by the fact that the interface constitutes a barrier for hot carrier transport, then the hot electron density available for any process in the MNPs should increase. This will be counteracted by the smaller depth available for absorption of light; the possible enhanced interface scattering should leave the energy inside the MNP. A net positive effect for the photochemical yield due to confinement is expected (see also the discussion in ref 42). Changes of hot electron-transfer dynamics at the special sites available on MNPs might contribute as well.

For the less likely case of direct primary excitation of the molecules, be it that this is the stronger excitation mechanism than hot electron transfer, be it that the molecules concerned do not sit on the MNPs but on the oxide support between the MNPs,[139,140,193] the only decisive effect will be field enhancement.

The MNP−support interface may also act as a barrier to heat conduction. The MNP might become hotter that way and stay hot longer, enabling thermal desorption from an overheated substrate. If such an effect can exist it will depend strongly on the support. For MNPs on alumina with its good thermal conductivity it might be unimportant.

In these considerations we assumed that the excitation densities are low. These concepts break down at high excitation densities, where mechanisms termed friction-induced desorption and DIMET[186] (see above) will take over. In the range of plasmon excitations, where the MNPs act as antennas collecting the energy into a small part of the surface area, photon fluences leading to low excitation densities if spread over the entire surface might suffice to lead into this range. This means that what happens on single-crystal surfaces with femtosecond laser pulses may happen on MNPs for much longer (or weaker) pulses. Under such conditions, transient transfer into negative-ion resonances might become more important. In addition, direct adsorbate excitations (plasmon enhanced) might also become more important than the substrate-mediated pathway. On the other hand, the friction-mediated mechanism could occur at lower photon fluences for MNPs as well (see also the discussion in ref 43).

These last considerations are applicable even without coupling between MNPs. They obviously would become aggravated for interacting MNP arrays since for them the plasmonic fields of the individual MNPs can couple nonlinearly and lead to strong spatial and temporal energy localization (hot spots) as discussed in section 2.3.3. It is very conceivable that such situations could lead to strong modifications of MNP photochemistry. No reports on such effects exist in the literature. Also, all measurements so far have been interpreted by the assumption that the photoactive species sit on the MNP surface.

Obviously, there can be different (and partly opposing) effects in photochemistry on MNPs compared to (the same) bulk material. The details are largely unclear; their disentanglement will require close interplay between careful preparation, detailed experimentation, and theoretical work.

3.2. Survey of Existing Work for Photochemistry on MNPs

3.2.1. Early Work and Related Experiments on Rough Surfaces

Insight into the influence of field enhancement in SERS prompted early considerations that these effects should be active in photoreactions as well. For example, Nitzan and Brus, who calculated the enhanced electric field on a small metallic sphere in connection with SERS in 1981,[194] argued for possible substantial enhancements of the photochemical yield. Das and Metiu described the enhancement of molecular fluorescence and photochemistry due to the presence of metal particles.[34] Enhancement factors of photochemical rates of more than 1 order of magnitude were calculated for a 20 nm Ag particle; however, the situation for molecules in direct contact with the particle could not be treated. The first experimental indication of a plasmon-enhanced photochemical reaction was reported in 1983 by Chen and Osgood[33] for the photodissociation of organometallic molecules (dimethyl cadmium) on cadmium spheres of 10−300 nm diameter using 257 nm light, i.e., in the region of the Cd plasmon. The $(CH_3)_2Cd$ adlayer was found to preferentially photodissociate on the poles of the electric field around the metal spheres leading to formation of ellipsoidal particles. No such development of ellipsoidal shapes was seen when

replacing Cd by gold, which does not possess a plasmon excitation in this energy range. Photodesorption of Na atoms from Na particles deposited on LiF(100) was the first direct observation of MNP field enhancement influencing a photochemical process.[195] The photodesorption yield peaked at 490 nm, which corresponds to the particle plasmon resonance. The conclusion of a nonthermal desorption mechanism was derived from the high kinetic energy of desorbing Na atoms (about 1.6 eV) and the negligible surface heating estimated from the low laser fluences used. The importance of electric field effects was reproduced by a theoretical study calculating the surface electromagnetic field as a function of particle size.[196] The study demonstrated that the energetics of the desorption is compatible with bond rupture of Na atoms at certain sites on the particles following a MGR-type mechanism.[164] In these works the definition of the MNPs and their surfaces might have been suboptimal, but they are important historically as well as conceptually.

The role of plasmon enhancement has also been shown for rough surfaces. Photodissociation of submonolayer $Mo(CO)_6$ adsorbed on Al films on quartz,[197] the photodesorption of NO, OCS, and SO_2 from roughened silver surfaces,[198−200] and the photodissociation of $Fe(CO)_5$ on Ag(111)[201] were studied. Although these experiments did not deal explicitly with MNPs, their results suggest that similar mechanisms should hold for the photochemistry on MNPs since enhancement of surface electromagnetic field is the relevant parameter in all cases.

3.2.2. Photochemistry on Defined MNPs

Photodissociation of Methane on Pd Nanoparticles. Photodissociation of methane physisorbed on Pd NPs is of particular interest as it shows a clear particle-size dependence for the interactions in the ground state as well as in the electronically excited state. Methane physisorbed on Pt(111),[202] Pd(111),[203] and Cu(111)[204] surfaces is readily dissociated into methyl and hydrogen by irradiation with a 193 nm (6.42 eV) ArF excimer laser. On Cu(111), methane photodissociation leads to ethylene formation.[204] These observations are surprising because light absorption in gaseous methane does not occur at wavelengths above 145 nm (8.55 eV). The peculiarity of the methane/transition-metal systems consists of the fact that methane on these surfaces is excited by a direct electronic transition localized within the adsorbate−substrate complex, as proved by polarization-dependent measurements.[205] This is in contrast to most of the usual surface photochemistry on metals and semiconductors at low excitation energies which is due to substrate-mediated excitations. The lowering of the excitation energy can be understood by an electronic interaction in the excited state resulting in hybridization of the excited 3s state of methane and the unoccupied states of the metal. The resulting hybrid state is much lower in energy than the molecular 3s state, explaining why excitation is possible by 6.42 eV photons.

On Pd NPs on a thin alumina film methane adsorbs weakly and thermally desorbs as molecule, as in the Pd(111) case. The interaction between methane and Pd NPs becomes stronger with increasing particle size as shown by the TPD results in Figure 12.[206] For large particles the desorption temperature slowly approaches the value for Pd(111). The long tail at higher temperatures can be attributed to the particle size distribution and the inhomogeneity of the surface structure of the Pd NPs, which contain (111) and (100) facets as well as edge and kink sites.[50] The size dependence of the methane−NP interaction in the ground state reflects the increase of the dispersion forces (van der Waals interaction) with increasing size due to the higher number of electrons available for the dynamic response in larger NPs. A similar trend in the methane−NP interactions has been reported recently for Pd NPs formed on MgO surfaces.[207] Irradiation of a CD_4 layer leads to photodissociation into CD_3 and D on the surface as well as to photodesorption of CD_4. Since CD_3 desorbs associatively upon heating in the presence of preadsorbed H, the degree of photodissociation can be detected by TPD of CD_3H; the TPD peak area of CD_3H is then proportional to the number of methyl groups formed by laser irradiation. Figure 13 shows a series of TPD results for CD_3H measured after 193 nm ArF laser irradiation (1.5×10^{19} photons/cm^2) onto CD_4-precovered Pd particles on alumina as a function of particle size. It is readily seen that the methyl formation rate increases with increasing particle size.

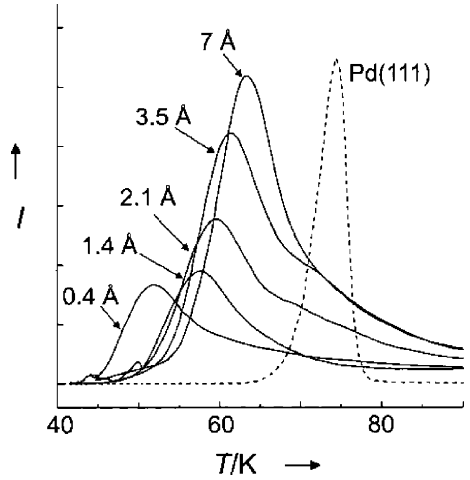

Figure 12. Series of CD_4 TPD spectra ($m/z = 20$; solid curves) from Pd nanoparticles of various sizes deposited on a thin $A1_2O_3$ film epitaxially grown on NiAl(110). The sample was exposed to 0.5 L CD_4 at 40 K (1 L = 10^{-6} Torr·s). The desorption peaks are due to molecular desorption, $CD_4(ads) \rightarrow CD_4(g)$. The numbers denote the total Pd coverages as a measure of the nanoparticle size. The dashed curve corresponds to a TPD spectrum of a Pd(111) single-crystal surface after exposure to 0.6 L CD_4 and is depicted on a different scale. Reprinted with permission from ref 206. Copyright 1999 Wiley−VCH Verlag GmbH.

The efficiency of the CD_4 photodesorption using the same irradiation can be derived from the TPD integrals of CD_4. Figure 14 shows a plot of the CD_3H formation ratio β and the CD_4 depletion ratio α as a function of the total Pd coverage. It is seen that methyl formation increases with particle size, whereas the depletion ratio decreases. This implies that the photodesorption is enhanced as the particle size is reduced whereas photodissociation is suppressed. The lower depletion ratio for the larger NPs has been attributed to a poisoning effect as a result of the increased methyl concentration.[202]

The photoexcitation mechanism of methane has been supported by ab initio calculations for CH_4/Pt_n and CH_4/Pd_n clusters by Akinaga et al.[208,209] The excited state responsible for dissociation to $CH_3 + H$ is formed from mixing of an antibonding Rydberg state of methane, localized 10 eV above the HOMO of gas phase methane, and unoccupied states of the metal. The excitation energy depends strongly on the cluster size because electron redistribution over the metal

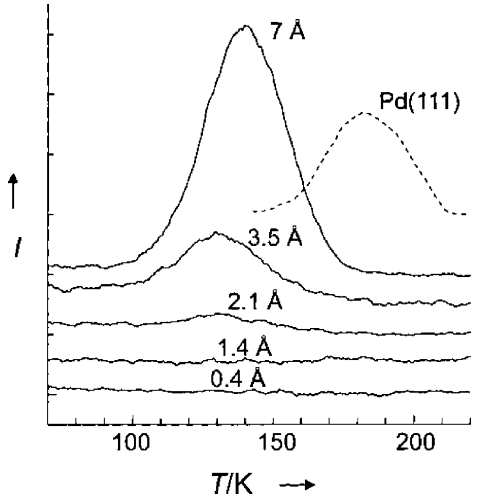

Figure 13. Series of CD_3H TPD spectra (m/z =19; solid curves) of 0.5 L CD_4 precovered Pd nanoparticles of various sizes after laser irradiation with 1.5×10^{19} photons per cm^2 at 193 nm. The desorption peaks are due to recombinative desorption, CD_3(ads) + H(ads) → CD_3H(g). The numbers denote the total Pd coverages as a measure of the nanoparticle size. The dashed curve corresponds to a TPD spectrum after irradiation of a Pd(111) single-crystal surface precovered with 1.1 L CD_4 and is depicted on a different scale. Reprinted with permission from ref 206. Copyright 1999 Wiley−VCH Verlag GmbH.

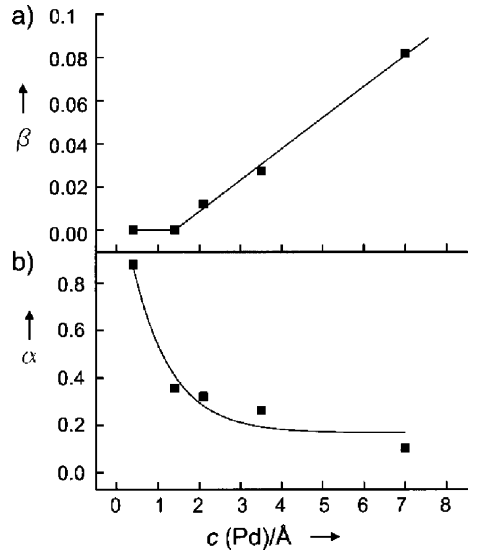

Figure 14. (a) Plot of the CD_3H formation ratio β ($\beta = B/A_0$; B = integrated TPD peak areas of CD_3H after irradiation, A_0 = integrated TPD peak area of initially adsorbed CD_4 before irradiation) as a function of the total Pd coverage c; (b) plot of the CD_4 depletion ratio α ($\alpha = 1 - A/A_0$; A_0 = integrated peak areas of CD_4 before irradiation, A = integrated peak areas of CD_4 after irradiation with 1.5×10^{19} photons per cm^2) as a function of the total Pd coverage. Total Pd coverages of 1.4, 2.1, 3.5, and 7 Å correspond to average nanoparticle sizes of 37, 49, 65, and 73 Å, respectively. Reprinted with permission from ref 206. Copyright 1999 Wiley−VCH Verlag GmbH.

cluster plays an important role in stabilizing this charge-transfer state. Further stabilization of the excited state can come from the image force.[210] The calculated excitation energy including image force effects results in 5.1 eV, which is accessible by a 6.4 eV photon. The methane−Pd NP system demonstrates the possibility to control competing photochemical paths by tuning the size and consequently the electronic structure of MNPs.

Photodesorption of NO and Site Conversion of CO on Pd Nanoparticles. A variety of adsorption sites exist on the surface of MNPs compared to single-crystal surfaces. Kampling et al. reported photodesorption of NO from amorphous and ordered Pd NPs on thin alumina films at 6.4 eV and found marked differences from the behavior on the flat Pd(111) surface, where NO photodesorption is absent.[211] The desorption efficiency increases with decreasing particle sizes below 8 nm. On amorphous Pd NPs a substantial amount of NO is only weakly bound, a characteristic which is well known from stepped Pd crystals. Such weakly bound NO shows a larger photodesorption cross section than the strongly chemisorbed NO on ordered NPs.

However, the final-state energy distributions of desorbing NO, as detected by REMPI, did not show strong size and morphology dependences. Three possible mechanisms were proposed to explain the observation: (i) desorption from low-coordinated Pd atoms, (ii) laser-induced spill over to the alumina support, and (iii) Pd particle sizes smaller than the mean free path of electrons. It was suggested that changes in the lifetimes of electronically excited states and modifications of the potential-energy surfaces as a function of particle size are responsible for the final state distributions and different photodesorption efficiencies.

TPD and IRAS were used to study adsorption site changes of CO bound to amorphous and crystalline Pd NPs on thin alumina films on NiAl(110) at 120 K after irradiation with UV laser light of $\lambda = 355$ nm.[212,213] Site changes from higher coordinated sites to on top positions were found which occurred only for nonequilibrium adsorbate structures. Such adsorbate configurations were prepared by annealing a CO-saturated surface to 300 K; they reveal a higher local adsorbate density in combination with vacant adsorption sites at on-top positions of the palladium. Site-exchange processes were observed to occur reversibly in a cycle of laser irradiation and annealing (to 250−300 K). The observed site changes were found to be strongly dependent on the CO adsorption structure as well as on the size and morphology of the Pd NPs. The effect of laser-induced repopulation was most pronounced for small NPs. As an explanation, the presence of a floating CO phase coupled via CO−CO repulsion was suggested to be responsible for the collective site changes. The site change effects would then be induced by fluctuations of the local electron density after laser irradiation. However, details of the size and morphology dependence of the initial electron dynamics are obscured by the complexity of the collective site-exchange processes and could not be resolved.

Very Recent Work: Water and NO on Ag NPs. Very recently, a first attempt to utilize the potential of time-dependent measurements on MNP-induced photochemistry has been made by the group of M. Wolf.[214] They investigated the photochemistry of water on laser-shaped Ag NPs supported on quartz (rather high coverage, estimated at around 50% of the surface area) by following the desorption of water by a femtosecond laser two-pulse correlation technique. They did not find any evidence for an influence of very short time scales in the dynamics leading to desorption; the desorption of H_2O was found to be purely phonon mediated. In the experiment the MNP lattice modes were resonantly heated by tuning the laser wavelength to the energy of the horizontal plasmon mode in the NPs and the molecules desorbed thermally. The MNP absorption spectra were found to red shift with water coverage; the

caused attenuation was small. On the basis of an approximate analysis the desorption temperature was estimated to 1000 K and the cooling time of the MNPs to around 500 ps. The analysis depends on the assumption that the observed processes occur on the Ag NPs, even though the adsorption energies of water on quartz and Ag are very similar and the entire surface is likely covered with water.

Also very recently, Wettergren et al. reported the effect of plasmon excitations on the photodesorption of NO from a graphite (0001) surface covered with Ag NPs.[215] Figure 15 shows the normalized initial yield of desorbing NO at

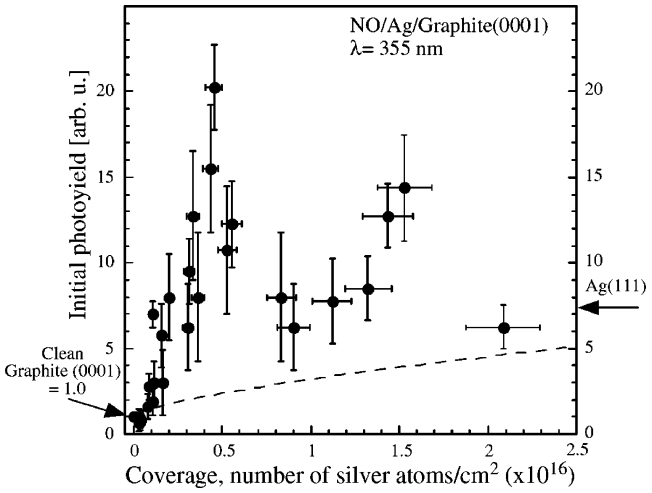

Figure 15. Initial yield for NO desorption from a graphite(0001) surface covered with Ag nanoparticles, normalized with respect to the pulse energy and NO coverage, as a function of Ag coverage. The dashed line shows the expected increase in the initial yield due to the increased silver nanoparticle area. The arrows mark the initial yield from clean graphite and the expected initial yield from an Ag(111) surface. Reprinted with permission from ref 215. Copyright 2005 Elsevier.

355 nm as a function of silver coverage from such graphite surfaces. Here the silver coverage was relatively small ($\leq$5.5% of the graphite surface) and the particle sizes were large (up to 133 nm long and 95 nm high). The data still show a clear increase in the yield as high as 20-fold with respect to the Ag-free surface. The maximum was attributed to the plasmon-related field enhancement and the concomitant increase of hot electron production. It should be noted that again both the particles and the support were covered by NO in the experimental situation.

The authors' group recently studied photodesorption of NO adsorbed on Ag NPs (mean size 8 nm) on thin alumina films on NiAl(110) by mass-selected time-of-flight spectra (MS-TOF) of desorbing NO from layers characterized by TPD.[216] NO was photodesorbed by nanosecond laser pulses at $h\nu = 3.5$ and 4.0 eV. Photodesorption cross sections were obtained from the fluence dependences of the integrated TOF signals of desorbing NO. Compared to Ag(111),[217,218] enhancement factors of 29 (3.5 eV) and 1.8 (4.0 eV) were found on the Ag NPs. The large enhancement at 3.5 eV is explained by resonant excitation of the Ag Mie plasmon which has also been seen in the 2PPE results.[108] Mean translational energies of NO were 700−800 K, considerably larger than for Ag(111) substrates, where ~490 K was measured.[218] This increase may be connected to increased hot electron lifetimes for the MNPs.

4. Summary and Outlook

There is no question that the size and morphology of MNPs strongly influence the photochemistry on their surfaces. MNPs may offer new adsorption sites and new electronic states, which are absent on single-crystal surfaces. The special photochemistry occurring on MNPs is related to these changes of electronic structure and geometrical parameters (which are, of course, correlated). Different ground and excited electronic states and their lifetimes then result in different dynamics and kinetics on nanostructured surfaces.

This survey has shown that the particular photophysical properties of MNPs are diverse and complicated, but as they have been investigated for a considerable time, the accumulated knowledge and understanding is appreciable. The confinement of excitations due to the small size of the MNPs is likely to increase the efficiency of photochemistry. The overwhelming importance of the plasmon excitation, when present, and of the concomitant field enhancement is very obvious; the time evolution following the excitation is understood in principle. The relevant parameters are generally clear, even though their magnitude, relative importance, and interplay are not understood in detail. What is still missing here is to perform all experiments on well-defined samples where size and morphology of the individual particles as well as their arrangement on the support are well determined. While, in principle, a bottom-up approach (build up by soft landing of mass-selected particles with subsequent in situ characterization) might appear more appealing, in practice the (now well-developed) procedures for preparing defined samples by vapor deposition seem to be more promising. Also, use of alloy NPs such as Au−Ag[122] may allow one to tailor plasmon enhancement with specific chemical selectivity for surface photoreactions of interest.

In comparison to the progress made in photophysics, work on the photochemistry on well-defined samples is very much in its beginning stage with the number of publications being quite small. Again, it will be of utmost importance to work with well-defined samples. Application of the highly developed laser techniques with their continuing extension to shorter pulse times will certainly be very fruitful.

The most promising approach will be combined photophysical and photochemical investigations using the same sample to exclude any influence of sample preparation on the transferability of results.

Unanswered questions abound. The relative contributions of the various sketched (and maybe of new) mechanisms have to be sorted out and explained and examined for low and high excitation densities. The contributions of plasmon enhancement and detailed influence of hot electron dynamics on the photochemical processes have to be examined for molecules in contact with the MNPs. A mere influence of the field enhancement for molecules not in contact with the MNPs may be important to induce reactions on the oxide. Such an antenna effect of MNPs may be usable to induce spill-over effects of hot electrons, where local injection of e−h pairs into a suitable oxide triggers photochemical reactivity on such oxides, possibly even allowing one to probe the length scale of such transfer processes. In all cases, the plasmonic coupling in an array of MNPs and the connected hotspot formation may lead to peculiar reactive situations. There is no question that this is an exciting research field and that interesting results can be expected soon.

5. Acknowledgments

We are grateful for support to the German Science Foundation within Priority Program SSP1093 (Dynamik von Elektronentransferprozessen an Grenzflächen), the German Israeli Foundation (Dynamics of Electronic Processes in a Confined Environment), the Fonds der Chemischen Industrie, and the NEDO International Joint Research Grant on Photon and Electron Controlled Surface Processes.

6. References

(1) *Laser Spectroscopy and Photochemistry on Metal Surfaces*; Dai, H.-L., Ho, W., Eds.; World Scientific: Singapore, 1995.
(2) Polanyi, J. C. *Science* **1987**, *236*, 680.
(3) Zare, R. N. *Science* **1998**, *279*, 1875.
(4) Campbell, C. T. *Surf. Sci. Rep.* **1997**, *27*, 1.
(5) Freund, H.-J. *Angew. Chem., Int. Ed. Engl.* **1997**, *36*, 452.
(6) Henry, C. R. *Surf. Sci. Rep.* **1998**, *31*, 231.
(7) Freund, H.-J. *Surf. Sci.* **2002**, *500*, 271.
(8) Bäumer, M.; Freund, H.-J. *Prog. Surf. Sci.* **1999**, *61*, 127.
(9) Henry, C. R. *Prog. Surf. Sci.* **2005**, *80*, 92.
(10) Kreibig U.; Vollmer, W. *Optical Properties of Metal Clusters*; Springer: Berlin, 1995.
(11) Ekardt, W. *Metal clusters*; Wiley: Chichester, 1999.
(12) *Metal Clusters at Surfaces−Structure, Quantum Properties, Physical Chemistry*; Meiwes-Broer, K.-H., Ed.; Springer: Berlin Heidelberg, 2000.
(13) Eberhardt, W. *Surf. Sci.* **2002**, *500*, 242.
(14) Schmid, G. *Clusters and colloids*: *from theory to applications*; VCH: Weinheim, 1994.
(15) Templeton, A. C.; Wuelfing, W. P.; Murray, R. W. *Acc. Chem. Res.* **2000**, *33*, 27.
(16) *Metal nanoparticles*: *synthesis, characterization, and applications*; Feldheim, D. L., Foss, C. A., Jr., Eds.; Marcel Dekker: New York, 2002.
(17) Bernhardt, T. M. *Int. J. Mass Spectrom.* **2005**, *243*, 1 and references therein.
(18) Heiz, U.; Schneider, W.-D. *J. Phys. D*: *Appl. Phys.* **2000**, *33*, R85.
(19) Wesendrup, R.; Schroder, D.; Schwarz, H. *Angew. Chem., Int. Ed.* **1994**, *33*, 1174.
(20) Bohme, D. K.; Schwarz, H. *Angew. Chem., Int. Ed.* **2005**, *44*, 2336.
(21) Socaciu, L. D.; Hagen, J.; Bernhardt, T. M.; Wöste, L.; Heiz, U.; Häkkinen, Landman, U. *J. Am. Chem. Soc.* **2003**, *125*, 10437.
(22) Wallace, W. T.; Whetten, R. L. *J. Am. Chem. Soc.* **2002**, *124*, 7499.
(23) Brown, L. A.; Rayner, D. M. *J. Chem. Phys.* **1998**, *109*, 2474.
(24) Lüttgens, G.; Pontius, N.; Bechthold, P. S.; Neeb, M.; Eberhardt, W. *Phys. Rev. Lett.* **2002**, *88*, 076102.
(25) Bromann, K.; Felix, C.; Brune, H.; Harbich, W.; Monot, R.; Buttet, J.; Kern, K. *Science* **1996**, *274*, 956.
(26) Jodicke, H.; Schaub, R.; Monot, R.; Buttet, J.; Harbich, W. *Surf. Sci.* **2001**, *475*, 109.
(27) Schaub, R.; Jodicke, H.; Brunet, F.; Monot, R.; Buttet, J.; Harbich, W. *Phys. Rev. Lett.* **2001**, *86*, 3590.
(28) Yamaguchi, W.; Ohashi, H.; Murakami, J. *Chem. Phys. Lett.* **2002**, *364*, 1.
(29) Yasumatsu, H.; Hayakawa, T.; Koizumi, S.; Kondow, T. *J. Chem. Phys.* **2005**, *123*, 124709.
(30) Yasumatsu, H.; Hayakawa, T.; Kondow, T. *J. Chem. Phys.* **2006**, *124*, 014701.
(31) Carroll, S. J.; Pratontep, S.; Streun, M.; Palmer, R. E.; Hobday, S.; Smith, R. *J. Chem. Phys.* **2000**, *113*, 7723.
(32) Link, S.; El-Sayed, M. A. *Annu. Rev. Phys. Chem.* **2003**, *54*, 331.
(33) Chen, C. J.; Osgood, R. M. *Phys. Rev. Lett.* **1983**, *50*, 1705.
(34) Das, P.; Metiu, H. *J. Phys. Chem.* **1985**, *89*, 4680.
(35) Spillover of adsorbed species. In *Proceedings of the International Symposium, Lyon-Villeurbanne, September 12−16, 1983*; Pajonk, G. M., Teichner, S. J., Germain, J. E., Eds.; Elsevier: Amsterdam, 1983.
(36) Knoesel, E.; Hotzel, A.; Wolf, M. *Phys. Rev. B* **1998**, *57*, 12812.
(37) Petek, H.; Ogawa, S. *Prog. Surf. Sci.* **1997**, *56*, 239.
(38) Petek, H.; Ogawa, S. *Annu. Rev. Phys. Chem.* **2002**, *53*, 507.
(39) Frischkorn, C. *Surf. Sci.* **2005**, *593*, 67.
(40) Gadzuk, J. W. *Chem. Phys.* **2000**, *251*, 87.
(41) Bonn, M.; Denzler, D. N.; Funk, S.; Wolf, M. *Phys. Rev. B* **2000**, *61*, 1101.
(42) Lisowski, M.; Loukakos, P. A.; Bovensiepen, U.; Stähler, J.; Gahl, C.; Wolf, M. *Appl. Phys. A* **2004**, *78*, 165.
(43) Zhdanov, V. P.; Kasemo, B. *J. Phys.: Condens. Matter* **2004**, *16*, 7131.
(44) Zhou, X.-L.; Zhu, X.-Y.; White, J. M. *Surf. Sci. Rep.* **1991**, *13*, 73.
(45) Zhu, X.-Y. *Annu. Rev. Phys. Chem.* **1994**, *45*, 113.
(46) Träger, F. *Appl. Phys. B* **2001**, *73*, 291 and references therein.
(47) Stietz, F. *Appl. Phys. A* **2001**, *72*, 381.
(48) Nilius, N.; Ernst, N.; Freund H.-J. *Phys. Rev. Lett.* **2000**, *84*, 3994.
(49) Benia, H.-M.; Nilius, N.; Freund, H.-J. *Surf. Sci.* **2006**, *600*, L128.
(50) Hansen, K. H.; Worren, T.; Stempel, S.; Laegsgaard, E.; Bäumer, M.; Freund, H.-J.; Besenbacher, F.; Stensgaard, I. *Phys. Rev. Lett.* **1999**, *83*, 4120.
(51) Kulawik, M.; Nilius, N.; Freund, H.-J. *Phys. Rev. Lett.* **2006**, *96*, 036103.
(52) Freund, H.-J.; Dillmann, B.; Ehrlich, D.; Hassel, M.; Jaeger, R. M.; Kuhlenbeck, H.; Ventrice, C. A., Jr.; Winkelmann, F.; Wohlrab, S.; Xu, C.; Bertrams, Th.; Brodde A.; Neddermeyer H. *J. Mol. Catal.* **1993**, *82*, 143.
(53) Bosbach, J.; Martin, D.; Stietz, F.; Wenzel, T.; Träger, F. *Appl. Phys. Lett.* **1999**, *74*, 2605.
(54) Wong, K.; Johansson, S.; Kasemo, B. *Faraday Discuss.* **1996**, *105*, 237.
(55) Jacobs, P. W.; Wind, S. J.; Ribeiro, F. H.; Somorjai, G. A. *Surf. Sci.* **1997**, *372*, L249.
(56) Bäumer, M.; Libuda, J.; Sandell, A.; Freund, H.-J.; Graw, G.; Bertrams, Th.; Neddermeyer, H. *Ber. Bunsen-Ges. Phys. Chem.* **1995**, *99*, 1381.
(57) Wertheim, G. K. *Z. Phys. B* **1987**, *66*, 53.
(58) Voisin, C.; Fatti, N. D.; Christofilos, D.; Vallée, F. *J. Phys. Chem. B* **2001**, *105*, 2264.
(59) Egelhoff, W. F., Jr. *Surf. Sci. Rep.* **1987**, *6*, 253.
(60) Wertheim, G. K.; DiCenzo, S. B.; Buchanan, D. N. E. *Phys. Rev. B* **1986**, *33*, 5384.
(61) Wertheim, G. K. *Z. Phys. D* **1989**, *12*, 319.
(62) Richter, B.; Kuhlenbeck, H.; Freund, H.-J.; Bagus, P. S. *Phys. Rev. Lett.* **2004**, *93*, 026805.
(63) Bäumer, M.; Libuda, J.; Freund, H.-J. In *Chemisorption and Reactivity on Supported Clusters and Thin Films*; Lambert, R. M., Pacchioni, G., Eds.; NATO ASI Series E 331; Kluwer: Dordrecht, 1997; p 61.
(64) Sandell, A.; Libuda, J.; Brühwiler, P. A.; Andersson, S.; Bäumer, M.; Maxwell, A. J.; Mårtensson, N.; Freund, H.-J. *Phys. Rev. B* **1997**, *55*, 7233.
(65) Klekamp, A.; Umbach, E. *Surf. Sci.* **1993**, *284*, 291.
(66) Hövel, H.; Grimm, B.; Pollmann, M.; Reihl, B. *Phys. Rev. Lett.* **1998**, *81*, 4608.
(67) Hövel, H.; Barke, I.; Boyen, H.-G.; Ziemann, P.; Garnier, M. G.; Oelhafen, P. *Phys. Rev. B* **2004**, *70*, 045424.
(68) Howard, A.; Clark, D. N. S.; Mitchell, C. E. J.; Egdell, R. G.; Dhanak, V. R. *Surf. Sci.* **2002**, *518*, 210.
(69) Tanaka, A.; Takeda, Y.; Nagasawa, T.; Sato, S. *Phys. Rev. B* **2003**, *67*, 033101.
(70) Tanaka, A.; Takeda, Y.; Imamura, M.; Sato, S. *Phys. Rev. B* **2003**, *68*, 195415.
(71) Chen, C. J. *Introduction to Scanning Tunneling Microscopy*; Oxford University Press: New York, 1993.
(72) Andres, R. P.; Bein, T.; Dorogi, M.; Feng, S.; Henderson, J. I.; Kubiak, C. P.; Mahoney, W.; Osifchin, R. G.; Reifenberger, R. *Science* **1996**, *272*, 1323.
(73) Hövel, H.; Barke, I. *New J. Phys.* **2003**, *5*, 31.1.
(74) Barke, I.; Hövel, H. *Phys. Rev. Lett.* **2003**, *90*, 166801.
(75) Hövel, H.; Barke, I. *Progr. Surf. Sci.* **2006**, *81*, 53.
(76) Nilius, N.; Kulawik, M.; Rust, H.-P.; Freund, H.-J. *Surf. Sci.* **2004**, *572*, 347.
(77) Wang, B.; Wang, K.; Lu, W.; Yang, J.; Hou, J. G. *Phys. Rev. B* **2004**, *70*, 205411.
(78) Quinn, J. J. *Phys. Rev.* **1962**, *126*, 1453.
(79) Anisimov, S. I.; Kapeliovich, B. L.; Perel′man, T. L. *Sov. Phys.-JETP* **1974**, *39*, 375.
(80) Guillon, C.; Langot, P.; Del Fatti, N.; Vallée, F. *New J. Phys.* **2003**, *5*, 13.1.
(81) Liebsch, A. *Phys. Rev. B* **1993**, *48*, 11317.
(82) Voisin, C.; Christofilos, D.; Del Fatti, N.; Vallée, F.; Prevel, B.; Cottancin, E.; Lerme, J.; Pellarin, M.; Broyer, M. *Phys. Rev. Lett.* **2000**, *85*, 2200.
(83) Del Fatti, N.; Vallée, F. *Appl. Phys. B* **2001**, *73*, 383.
(84) Del Fatti, N.; Vallée, F.; Flytzanis, C.; Hamanaka, Y.; Nakamura, A. *Chem. Phys.* **2000**, *251*, 215.
(85) Kawabata, A.; Kubo, R. *J. Phys. Soc. Jpn.* **1966**, *21*, 1765.
(86) Quijada, M.; Díez Muiño, R.; Echenique, P. M. *Nanotechnology* **2005**, *16*, S176.
(87) Pitarke, J. M.; Zhukov, V. P.; Keyling, R.; Chulkov, E. V.; Echenique, P. M. *ChemPhysChem* **2004**, *5*, 1284.
(88) Echenique, P. M.; Berndt, R.; Chulkov, E. V.; Fauster, Th.; Goldmann, A.; Höfer, U. *Surf. Sci. Rep.* **2004**, *52*, 219.
(89) Merschdorf, M.; Kennerknecht, C.; Willig, K.; Pfeiffer, W. *New J. Phys.* **2002**, *4*, 95.

(90) Merschdorf, M.; Pfeiffer, W.; Voll, S.; Gerber, G. *Phys. Rev. B* **2003**, *68*, 155416.
(91) Perakis, I. E.; Shahbazyan, T. V. *Surf. Sci. Rep.* **2000**, *40*, 1.
(92) Zhukov, V. P.; Aryasetiawan, F.; Chulkov, E. V.; Echenique, P. M. *Phys. Rev. B* **2002**, *65*, 115116.
(93) Zhukov, V. P.; Aryasetiawan, F.; Chulkov, E. V.; Gurtubay, I. G.; Echenique, P. M. *Phys. Rev. B* **2001**, *64*, 195122.
(94) Aeschlimann, M.; Bauer, M.; Pawlik, S.; Knorren, R.; Bouzerar, G.; Bennemann, K. H. *Appl. Phys. A: Mater. Sci. Process.* **2000**, *71*, 485.
(95) Faraday, M. *Philos. Trans. R. Soc. London* **1857**, *147*, 145.
(96) Molina, R. A.; Weinmann, D.; Jalabert, R. A. *Phys. Rev. B* **2002**, *65*, 155427.
(97) Simon, M.; Träger, F.; Assion, A.; Lang, B.; Voll, S.; Gerber, G. *Chem. Phys. Lett.* **1998**, *296*, 579.
(98) Bosbach, J.; Hendrich, C.; Stietz, F.; Vartanyan, T.; Träger, F. *Phys. Rev. Lett.* **2002**, *89*, 257404.
(99) Lazzari, R.; Roux, S.; Simonsen, I.; Jupille, J.; Bedeaux, D.; Vieger, J. *Phys. Rev. B* **2002**, *65*, 235424.
(100) Berciaud, S.; Cognet, L.; Tamarat, P.; Lounis, B. *Nano Lett.* **2005**, *5*, 515.
(101) Ertel, K.; Kohl, U.; Lehmann, J.; Merschdorf, M.; Pfeiffer, W.; Thon, A.; Voll, S.; Gerber, G. *Appl. Phys. B* **1999**, *68*, 439.
(102) Merschdorf, M.; Pfeiffer, W.; Thon, A.; Voll, S.; Gerber, G. *Appl. Phys. A* **2000**, *71*, 547.
(103) Lehmann, J.; Merschdorf, M.; Pfeiffer, W.; Thon, A.; Voll, S.; Gerber, G. *J. Chem. Phys.* **2000**, *112*, 5428.
(104) Lehmann, J.; Merschdorf, M.; Pfeiffer, W.; Thon, A.; Voll, S.; Gerber, G. *Phys. Rev. Lett.* **2000**, *85*, 2921.
(105) Merschdorf, M.; Kennerknecht, C.; Pfeiffer, W. *Phys. Rev. B* **2004**, *70*, 193401.
(106) Kennerknecht, C.; Hövel, H.; Merschdorf, M.; Voll, S.; Pfeiffer, W. *Appl. Phys. B* **2001**, *73*, 425.
(107) Cinchetti, M.; Valdaitsev, D. A.; Gloskovskii, A.; Oelsner, A.; Nepiko, S. A.; Schoenhense, G. *J. Electron Spectrosc. Relat. Phenom.* **2004**, *137*−*140*, 249.
(108) Evers, F.; Rakete, C.; Watanabe, K.; Menzel, D.; Freund, H.-J. *Surf. Sci.* **2005**, *593*, 43.
(109) Fauster, Th.; Steinmann, W. In *Photonic Probes of Surfaces*; Halevi, P., Ed.; Elsevier: Amsterdam, 1995 and work cited therein.
(110) Harris, C. B.; Ge, N.-H.; Lingle, R. L., Jr.; McNeil, J. D.; Wong, C. M. *Annu. Rev. Phys. Chem.* **1997**, *48*, 711.
(111) Osgood, R. M., Jr.; Wang, X. *Solid State Phys.* **1998**, *51*, 1.
(112) Zhu, X.-Y. *Annu. Rev. Phys. Chem.* **2002**, *53*, 221.
(113) Zhu, X.-Y. *Surf. Sci. Rep.* **2004**, *56*, 1 and references therein.
(114) Busolt, U.; Cottancin, E.; Röhr, H.; Socaciu, L.; Leisner, T.; Wöste, L. *Appl. Phys. B* **1999**, *68*, 453.
(115) Kubo, A.; Onda, K.; Petek, H.; Sun, Z.; Jung, Y. S.; Kim, H. K. *Nano Lett.* **2005**, *5*, 1123.
(116) Schmidt, Th.; Groh, U.; Fink, R.; Umbach, E.; Schaff, O.; Engel, W.; Richter, B.; Kuhlenbeck, H.; Schlögl, R.; Freund, H.-J.; Bradshaw, A. M.; Preikszas, D.; Hartel, P.; Spehr, R.; Rose, H.; Lilienkamp, G.; Bauer E.; Benner G. *Surf. Rev. Lett.* **2002**, *9*, 223.
(117) Drachsel, W.; Adelt, M.; Nilius, N.; Freund, H.-J. *J. Electron Spectrosc. Relat. Phenom.* **2002**, *122*, 239.
(118) Berndt, R. In *Scanning Probe Microscopy*; Wiesendanger, R., Ed.; Springer: Berlin, 1998; p 97.
(119) Nilius, N.; Coerper, A.; Bozdech, G.; Ernst, N.; Freund, H.-J. *Prog. Surf. Sci.* **2001**, *67*, 99.
(120) Nilius, N.; Ernst, N.; Freund, H.-J. *Surf. Sci.* **2001**, *478*, L327.
(121) Nilius, N.; Ernst, N.; Freund, H.-J.; *Chem. Phys. Lett.* **2001**, *349*, 351.
(122) Benten, W.; Nilius, N.; Ernst, N.; Freund, H.-J. *Phys. Rev. B* **2005**, *72*, 045403.
(123) Nilius, N.; Ernst, N.; Freund, H.-J. *Phys. Rev. B* **2002**, *65*, 115421.
(124) Benia, H.-M.; Nilius, N.; Freund, H.-J. *Surf. Sci.* **2006**, *600*, 128.
(125) Futamata, M.; Maruyama, Y.; Ishikawa, M. *J. Mol. Struct.* **2005**, *735-736*, 75.
(126) Nilius, N.; Benia, H.-M.; Salzemann, C.; Rupprechter, G.; Freund, H.-J.; Brioude, A.; Pileni, M.-P. *Chem. Phys. Lett.* **2005**, *413*, 10.
(127) Imura, K.; Nagahara, T.; Okamoto, H. *Chem. Phys. Lett.* **2004**, *400*, 500.
(128) Schatz, G. C.; Van Duyne, R. P. In *Handbook of Vibrational Spectroscopy*; Chalmers, J. M., Grifliths, P. R., Eds.; Wiley: New York, 2002; Vol. 1, p 759.
(129) Zou, S.; Schatz, G. C. *Chem. Phys. Lett.* **2005**, *403*, 62.
(130) Stockman, M. I. *Phys. Rev. Lett.* **2000**, *84*, 1011.
(131) Stockman, M. I.; Faleev, S. V.; Bergman, D. J. *Phys. Rev. Lett.* **2001**, *87*, 167401.
(132) Stockman, M. I. *Chem. Phys.* **2005**, *318*, 156.
(133) Barnes, W. L.; Dereux, A.; Ebbesen, T. W. *Nature* **2003**, *424*, 824.
(134) Van Duyne, R. P. *Science* **2004**, *306*, 985.
(135) Okamoto, T. *J. Spectrosc. Soc. Jpn.* **2005**, *54*, 225.
(136) Ozbay, E. *Science* **2006**, *311*, 189.
(137) Andrew, P.; Barnes, W. L. *Science* **2004**, *306*, 1002.
(138) Nie, S.; Emory, S. R. *Science* **1997**, *275*, 1102.
(139) Xu, H.; Bjerneld, E. J.; Käll, M.; Börjesson, L. *Phys. Rev. Lett.* **1999**, *83*, 4357.
(140) Michaels, A. M.; Jiang, J.; Brus, L. *J. Phys. Chem. B* **2000**, *104*, 11965.
(141) Su, K.-H.; Wei, Q.-H.; Zhang, X.; Mock, J. J.; Smith, D. R.; Schultz, S. *Nano Lett.* **2003**, *3*, 1087.
(142) Rechberger, W.; Hohenau, A.; Leitner, A.; Krenn, J. R.; Lamprecht, B.; Aussenegg, F. R. *Opt. Commun.* **2003**, *220*, 137.
(143) Gunnarsson, L.; Rindzevicius, T.; Prikulis, J.; Kasemo, B.; Käll, M.; Zou, S.; Schatz, G. *J. Phys. Chem. B* **2005**, *109*, 1079.
(144) Hövel, H.; Fritz, S.; Hilger, A.; Kreibig, U.; Vollmer, M. *Phys. Rev. B* **1993**, *48*, 18178.
(145) Persson, B. N. J. *Surf. Sci.* **1993**, *281*, 153.
(146) Brandt, T.; Hoheisel, W.; Iline, A.; Stietz, F.; Träger, F. *Appl. Phys. B* **1997**, *65*, 793.
(147) Stietz, F.; Träger, F. *Phil. Magn. B* **1999**, *79*, 1281.
(148) Iline, A.; Simon, M.; Stietz, F.; Träger, F. *Surf. Sci.* **1999**, *436*, 51.
(149) Pinchuk, A.; Kreibig, U. *New J. Phys.* **2003**, *5*, 151.
(150) Pinchuk, A.; Kreibig, U.; Hilger, A. *Surf. Sci.* **2004**, *557*, 269.
(151) Hendrich, C.; Bosbach, J.; Stietz, F.; Hubenthal, F.; Vartanyan, T.; Träger, F. *Appl. Phys. B* **2003**, *76*, 869.
(152) Garcia, M. A.; De la Venta, J.; Crespo, P.; LLopis, J.; Penadés, S.; Fernández, A.; Hernando, A. *Phys. Rev. B* **2005**, *72*, 241403.
(153) Bauer, C.; Abid, J.-P.; Girault, H. H. *J. Phys. Chem. B* **2006**, *110*, 4519.
(154) Park, S. Y.; Stroud, D. *Phys. Rev. Lett.* **2005**, *94*, 217401.
(155) Hall, R. B. *J. Phys. Chem.* **1987**, *91*, 1007.
(156) Ready, J. F. *Effects of High-Power Laser Radiation*; Academic Press: New York, 1971.
(157) Simpson, C. J. S. M.; Hardy, J. P. *Chem. Phys. Lett.* **1986**, *130*, 175.
(158) Watanabe, K.; Lin, M. C.; Gruzdkov, Y. A.; Matsumoto, Y. *J. Chem. Phys.* **1996**, *104*, 5974.
(159) Wedler G.; Ruhmann, H. *Surf. Sci.* **1982**, *121*, 464.
(160) Busch, D. G.; Gao, S.; Pelak, R. A.; Booth, M. F.; Ho, W. *Phys. Rev. Lett.* **1995**, *75*, 673.
(161) Ho, W. *J. Phys. Chem.* **1996**, *100*, 13050.
(162) Hicks, J. M.; Urbach, L. E.; Plummer, E. W.; Dai, H.-L. *Phys. Rev. Lett.* **1988**, *61*, 2588.
(163) Bourguignon, B.; Carre, S.; Büchner, M.; Henry, C. R. *Chem. Phys. Lett.* **1998**, *287*, 40.
(164) Götz, T.; Bergt, M.; Hoheisel, W.; Träger, F.; Stuke, M. *Appl. Phys. A* **1996**, *63*, 315.
(165) Stietz, F.; Stuke, M.; Viereck, J.; Wenzel, T.; Träger, F. *Surf. Sci.* **1997**, *389*, L1153.
(166) Domingues, G.; Voltz, S.; Joulain, K.; Greffet, J.-J. *Phys. Rev. Lett.* **2005**, *94*, 085901.
(167) Wenzel, T.; Bosbach, J.; Stietz, F.; Träger, F. *Surf. Sci.* **1999**, *432*, 257.
(168) Stietz, F.; Bosbach, J.; Wenzel, T.; Vartanyan, T.; Goldmann, A.; Träger, F. *Phys. Rev. Lett.* **2000**, *84*, 5644.
(169) Vartanyan, T.; Bosbach, J.; Stietz, F.; Träger, F. *Appl. Phys. B* **2001**, *73*, 391.
(170) Murakoshi, K.; Tanaka, H.; Sawai, Y.; Nakato, Y. *J. Phys. Chem. B* **2002**, *106*, 3041.
(171) Garcia de Abajo, F. J. *J. Quant. Spectrosc. Radiat. Transfer* **2004**, *89*, 3.
(172) Wong, V.; Ratner, M. A. *Phys. Rev. B* **2006**, *73*, 075416.
(173) Favazza, C.; Trice, J.; Krishna, H.; Kalyanaraman, R.; Sureshkumar, R. *Appl. Phys. Lett.* **2006**, *88*, 153118.
(174) DIET-8: Proceedings of the Eighth International Workshop on Desorption Induced by Electronic Transitions; San Alfonso, Long Branch, NJ, Sept 27−Oct 1, 1999; Madey, T., Zimmermann, F. M., Bartynski, R. A., Eds.; *Surf. Sci.* **2000**, *451* (1−3).
(175) DIET-9: Proceedings of the Ninth International Workshop on Desorption Induced by Electronic Transitions, Aussois, France, Jun 1−4, 2002; Raseev, G., Dujardin, G., Eds.; *Surf. Sci.* **2002**, *528* (1−3).
(176) DIET-10: Proceedings of the Tenth International Workshop on Desorption Induced by Electronic Transitions, Susono, Japan, Nov 8−11, 2004; Tanimura, K., Ueba, H., Eds.; *Surf. Sci.* **2005**, *593* (1−3).
(177) Menzel, D.; Gomer, R. *J. Chem. Phys.* **1964**, *41*, 3311.
(178) Redhead, P. A. *Can. J. Phys.* **1964**, *42*, 886.
(179) Feulner P.; Menzel D. In *Laser Spectroscopy and Photochemistry on Metal Surfaces*; Dai, H.-L., Ho, W., Eds.; World Scientific: Singapore, 1995; Chapter 16, p 627.
(180) Menzel, D.; Feulner, P. *J. Phys. Condens. Matter* **2001**, *13*, 11249.
(181) Zimmermann, F. M.; Ho, W. *Surf. Sci. Rep.* **1995**, *22*, 127.
(182) Wurth, W.; Menzel, D. *Chem. Phys.* **2000**, *251*, 141.
(183) Schulz, G. J. *Rev. Mod. Phys.* **1973**, *45*, 378.

(184) Sanche, L. *J. Phys. B* **1990**, *23*, 1597.
(185) Illenberger, E. In *Photoionization and Photodetachment*; Ng, C.-Y., Ed.; Advanced Series in Physical Chemistry 10B; World Scientific: Singapore, 2000; Part II, p 1063.
(186) Brandyge, M.; Hedegård, P.; Heinz, T. F.; Misewich, J. A.; Newns, D. M. *Phys. Rev. B* **1995**, *52*, 6042.
(187) Misewich, J. A.; Heinz, T. F.; Newns, D. M. *Phys. Rev. Lett.* **1992**, *68*, 25.
(188) Misewich, J. A.; Heinz, T. F.; Newns, D. M. *Phys. Rev. Lett.* **1992**, *68*, 3727.
(189) Bohnen, K. P.; Kiwi, M.; Suhl, H. *Phys. Rev. Lett.* **1975**, *34*, 1512.
(190) Nourtier, A. *J. Phys.* (*Paris*) **1977**, *38*, 479.
(191) Kittel, C. *Quatum Theory of Solids*; Wiley: New York, 1963; Chapter 6.
(192) Weick, G.; Molina, R. A.; Weinmann, D.; Jalabert, R. A. *Phys. Rev. B* **2005**, *72*, 115410.
(193) Futamata, M.; Maruyama, Y.; Ishikawa, M. *J. Phys. Chem. B* **2004**, *108*, 13119.
(194) Nitzan, A.; Brus, L. E. *J. Chem. Phys.* **1981**, *75*, 2205.
(195) Hoheisel, W.; Jungmann, K.; Vollmer, M.; Weidenauer, R.; Träger, F. *Phys. Rev. Lett.* **1988**, *60*, 1649.
(196) Monreal, R.; Apell, S. P. *Phys. Rev. B* **1990**, *41*, 7852.
(197) Wolf, M.; Zhu, X.-Y.; White, J. M. *J. Chem. Phys.* **1992**, *97*, 7015.
(198) Kidd, R. T.; Meech, S. R.; Lennon, D. *Chem. Phys. Lett.* **1996**, *262*, 142.
(199) Kidd, R. T.; Lennon, D.; Meech, S. R. *J. Chem.* **2000**, *113*, 8276.
(200) Burke, D. J.; Vondrak, T.; Meech, S. R. *Surf. Sci.* **2005**, *585*, 123.
(201) Sato, S.; Tanaka, S. *Appl. Surf. Sci.* **1998**, *135*, 83.
(202) Matsumoto, Y.; Gruzdkov, Y. A.; Watanabe, K.; Sawabe, K. *J. Chem. Phys.* **1996**, *105*, 4775.
(203) Watanabe, K.; Matsumoto, Y. *Surf. Sci.* **1997**, *390*. 250.
(204) Watanabe, K.; Matsumoto, Y. *Surf. Sci.* **2000**, *454*, 262.
(205) Watanabe, K.; Sawabe, K.; Matsumoto, Y. *Phys. Rev. Lett.* **1996**, *76*, 1751.
(206) Watanabe, K.; Matsumoto, Y.; Kampling, M.; Al-Shamery, K.; Freund, H.-J. *Angew. Chem., Int. Ed. Engl.* **1999**, *38*, 2192.
(207) Tait, S. L.; Dohnalek, Z.; Campbell, C. T.; Kay, B. D. *Surf. Sci.* **2005**, *591*, 90.
(208) Akinaga, Y.; Taketsugu, T.; Hirao, K. *J. Chem. Phys.* **1997**, *107*, 415.
(209) Akinaga, Y.; Taketsugu, T.; Hirao, K. *J. Chem. Phys.* **1998**, *109*, 11010.
(210) Jennison, D. R. Personal communication.
(211) Kampling, M.; Al-Shamery, K.; Freund, H.-J.; Wilde, M.; Fukutani, K.; Murata, Y. *Phys. Chem. Chem. Phys.* **2002**, *4*, 2629.
(212) Wille, A.; Haubitz, St.; Al-Shamery, K. *Chem. Phys. Lett.* **2003**, *367*, 609.
(213) Wille, A.; Al-Shamery, K. *Surf. Sci.* **2003**, *528*, 230.
(214) Kwiet, S.; Starr, D. E.; Grujic, A.; Wolf, M.; Hotzel, A. *Appl. Phys. B* **2005**, *80*, 115.
(215) Wettergren, K.; Kasemo, B.; Chakarov, D. *Surf. Sci.* **2005**, *593*, 235.
(216) Watanabe, K.; Kim, K. H.; Menzel, D.; Freund, H.-J. Manuscript in preparation.
(217) So, S. K.; Franchy, R.; Ho, W. *J. Chem. Phys.* **1991**, *95*, 1385.
(218) Vondrak, T.; Burke, D. J.; Meech, S. R. *Chem. Phys. Lett.* **2000**, *327*, 137.

CR050167G